FINITE ELEMENT ANALYSIS OF UNEXPECTED FAILURE OF LAKE-ICE UNDER LOADS MOVING AT CRITICAL VELOCITY

By

Ángel L. Quintero Cartagena

A thesis submitted in partial fulfillment of the requirements for the degree of

MASTER OF SCIENCE

in

MECHANICAL ENGINEERING

UNIVERSITY OF PUERTO RICO
MAYAGÜEZ CAMPUS

July 2012

Approved by:

Vijay K. Goyal, Ph.D. President, Graduate Committee	Date
Ricky Valentín, Ph.D. Member, Graduate Committee	Date
Stefano Leonardi, Ph.D. Member, Graduate Committee	Date
Gustavo Gutierrez, Ph.D. Chairperson of the Department	Date
Anand D. Sharma, Ph.D. Representative of Graduate Studies	Date

ABSTRACT

Through this work we predicted the unexpected failures of lake-ice under the effect of moving loads at critical velocity using finite element analysis. The main motivation was to solve the unexpected failure of the lake-ice at the Lake Ladoga during a military operation of the World War II named *"The Siege of Leningrad"* where it remained unclear why the slowly moving and heavy trucks did not break the ice, while rapidly moving and lighter trucks did. One possibility could be explained using the concept of critical velocity, being this the focal point of this work. We developed beam and plate viscoelastically supported models and the results produced the exact solution when compared to metal structures with moving loads and similar geometric and boundary scenarios. We showed that indeed the trucks reached the critical velocity on their way back, being this the main cause of the unexpected lake-ice failure; hence, resonance regimes were present causing instability and therefore loss of the structural stiffness of the lake-ice. Thus, we developed a novel approach to predict the unexpected lake-ice failure at critical velocity using the finite element analysis and we propose the first promising explanation for the *"Road of life"* at Lake Ladoga. The solved mystery is that the slowly moving heavy trucks did not break the lake-ice, but once the cargo was delivered, the lighter trucks drove back at higher speeds reaching velocities near the critical, creating unexpected failure of the lake-ice.

RESUMEN

A través de esta investigación predicimos la falla imprevista de lagos congelados bajo el efecto de cargas en movimiento a velocidad crítica, usando análisis de elementos finitos. La motivación primordial es resolver la falla imprevista de hielo en el Lago Ladoga durante la operación militar de la Segunda Guerra Mundial llamada *"The Siege of Leningrad"*, donde permanece incierto el porqué camiones lentos y pesados no quebraban en el hielo, mientras que camiones rápidos y livianos lo hacían. Una posible explicación se obtiene usando el concepto de velocidad crítica, siendo este el enfoque principal de este trabajo. Para esto fueron desarrollados los modelos con fundación elástica y viscoelástica de vigas y platos, y los resultados produjeron la solución exacta cuando se compararon con estructuras de metal con cargas en movimiento con geometría y condiciones de borde similares. Demostramos que los camiones alcanzaron la velocidad crítica en su regreso, siendo ésta la causa principal de la falla imprevista del lago congelado; por lo tanto, la resonancia estuvo presente causando la inestabilidad y la pérdida de rigidez estructural del hielo. Por lo tanto, desarrollamos un enfoque innovador para predecir la falla imprevista de lagos congelados a velocidad crítica usando el análisis de elementos finitos y proponemos la primera explicación contundente para la *"Ruta de la vida"* en el Lago Ladoga. La respuesta a este misterio es que los camiones lentos y pesados no quebraban el hielo, pero una vez la carga era entregada, estos camiones livianos regresaban a alta velocidades alcanzando velocidades cerca de la crítica, creando así la falla imprevista del hielo del lago.

DEDICATION

I dedicate this work...

First to Yahveh, the Almighty God, who has strengthened me throughout my life towards the pursuit of my goals;

Secondly, to my family. To Nery, my mother, who has instilled in me the desire to be a professional;

to Ángel Luis, my father, who has taught me by his example, that there is no excuse greater than the will to succeed;

and to Esther, my sister, who has always challenged me to reach for my dreams through her understanding of my personality;

Finally, I dedicate this to my beloved wife, Yaritza, for having been the best companion I could hope for through this journey.

ACKNOWLEDGMENTS

First, I want to thank God because through His will we are given the privilege of life. Next, I want to thank my parents for their unconditional love and support and my family, in general. I also would like to thank my wife, Yaritza González, for her patience and unconditional support throughout this thesis.

I am also indebted, and say my heartily thanks, to Dr. Vijay K. Goyal for the confidence he has always shown and for all these years for allowing me to be his graduate student. His unstinting support and guidance has always remained the key factor in my success. Once again, I want to thank Dr. Goyal also for providing me with this opportunity to take this next step in my career.

I want to thank Innovations in Research & Engineering (A29IRE), small business located in PR, for their support throughout this work. I found invaluable the theoretical and computational help they provided.

I would like to deeply thank Dr. Nicholas Nechitailo from Naval Surface Warfare Center Dalghren Division for his inputs and technical insights were invaluable. He was the one who first asked us the question: "Why is that the slowly moving heavy trucks, fully loaded with supplies, did not crack the ice in their way to Leningrad; however, once the cargo was delivered, on its way back to Leningrad, the unloaded trucks traveling faster in order to escape Axis bombardment would often break the lake-ice and sink?" We are thankful that Dr. Nechitailo would trust us with this project.

I cannot leave behind my colleague graduate students Sergio Candelario and Emmanuel Irizarry who greatly helped me during my thesis. A million thanks.

Angel

TABLE OF CONTENTS

LIST OF FIGURES

List of Symbols

A	Cross-sectional area
D	Plate flexural rigidity
E	Young modulus of elasticity
I	Second moment of inertia
F	Force
F^e	Equivalent nodal force of the element e
L	Structure length
$N_{1,2}$	Real numbers
P	Moving load
R	Residues at four simple poles
S	Compressive force
S_{cr}	Critical compressive force
b	Structure width
c	Damping coefficient
c_1	Deflection Amplitude
e	Element where the force is applied
f	Frequency
$\bar{f}$	Frequency of moving harmonic load
f_{cr}	Critical frequency
f_{cr0}	Critical frequency of a stationary harmonic load
g	Gravity constant
h	Structure thickness
k	Spring Constant
ℓ_e	Length of a element
t	Time variable
t_{st}	Time step
Δt	Time interval
v	Velocity
v_{cr}	Critical velocity
w	Transverse deflection
w_{st}	Static deflection
x_p	Position of the load at any time
x, y, z	Cartesian coordinates
α, β	Newmark time integration scheme stability and accuracy parameters
Δ	Plate deflection
λ	Static wave characteristic, $(k/4EI)^{1/4}$
ν	Poissons ratio
ϕ	Shape function

ρ	Ice density
ρ_w	Water density
ϑ	Weight function
ξ	Transformed field of moving space, $(x - vt)$

CHAPTER 1.
PRELIMINARY REMARKS

Through this work we plan on studying the unexpected failure of ice subject to a moving load using the concept of critical velocity and the finite element method (FEM). The structure being analyzed is an ice resting on calm lake water and it is subject to a moving load on top of the ice. We plan on making two water-ice system models: (i) beam model, (ii) and plate model. Both models are will be subject to an identical geometry and the same moving load, and the ice will be resting over a viscoelastic medium which best models the water under the ice. All results will be validated against results available in the literature. In short, we will develop a finite element based solution to predict the ice rupture under moving loads on frozen lakes and attempt to explain the unsolved mystery of the *"Road of Life"* at Lake Ladoga.

1.1 Motivation

The dynamic behavior of ice-structures subject to moving loads remains a field of interest for the Department of Transportation. This field has many applications such as, but not limited to, train's rails, bridges and high-speed projectile launchers. The concept of critical velocity approach was first introduced in 1927 by Timoshenko [1]. He stated that at critical velocity conditions, the structure becomes unstable and buckling takes place. Similar conclusions later were stated by Kenney [2], which presented an analytical solution for constant velocity of a moving load on beams resisting over an elastic foundation. Similarly, Nechitailo and Lewis [3] used ABAQUS to visualize the deformation behavior of the deflections and stresses.

The main motivation of this research is to solve the unexpected failure of the ice at the Lake Ladoga, shown in Figure 1–1, during one of the most destructive military

Figure 1–1: "Road of Life "at Lake Ladoga.

operation of the World War II named *"The Siege of Leningrad"*. This operation was performed for the Axis power, placing Leningrad under siege conditions with the unsuccessful mission of capture Leningrad. During this operation, Lake Ladoga was the only access to the besieged city, creating the so called *"Road of Life"*. This road was used by military trucks to transport supplies into Leningrad over the frozen lake during the winter, and boats during the summer. What really caught our attention was that the slowly moving heavy trucks, fully loaded with supplies, did not crack the ice in their way to Leningrad; however, once the cargo was delivered, on its way back to Leningrad, the unloaded trucks traveling faster in order to escape Axis bombardment would often break the lake-ice and sink. It was not clear why the slowly moving and heavy trucks did not break the ice, while rapidly moving and lighter trucks did. One possibility could be explained using the concept of critical velocity, being this the focal point of this work.

Achieving a possible explanation for the previously stated situation was the major motivation of this work although the applications of this work are various. An analytical solution, which for a few idealized cases may exist, is cumbersome and a numerical technique becomes a promising technique to predict the behavior. Here, we plan on using the finite element method as the numerical technique.

1.2 Problem Description

Throughout this work, we will focus our attention to the ice as the structural component and the still water upon which it is resting will be added as distributed spring-dampers over the domain. In other words, the still water will be modeled as a viscoelastic material medium under the ice. The moving load is a assumed as a point loads, although the four tires should be modeled as two moving point loads for the beam model and four moving points for the plate model.

The finite element model will focus on try to capture the wave propagation to predict the critical velocity. In this context, we will be able to better understand the behavior of the critical velocity as it enters in resonance with the ice-structure and producing the ice-cracking.

Figure 1–2 captures the problem describes in the above paragraph. The light-weight truck is moving with a constant velocity v, over a layer of the frozen ice resting on the still water, from left to right.

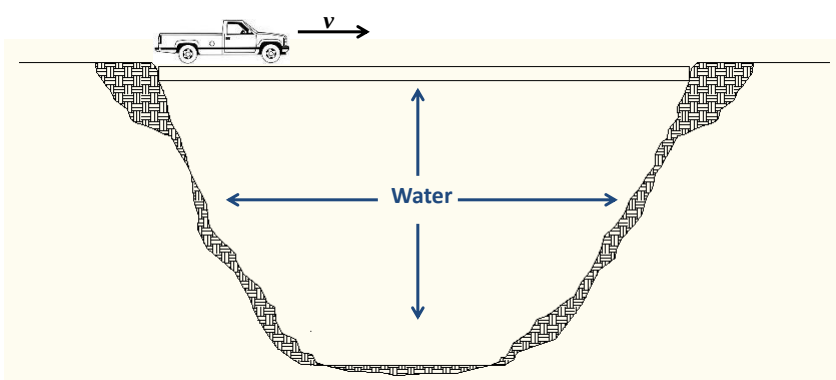

Figure 1–2: Moving vehicle over the frozen lake.

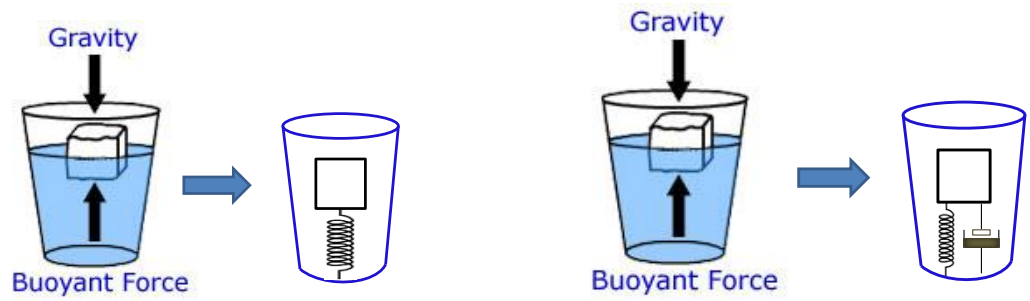

Figure 1–3: Water as elastic and viscoelastic foundations.

As mentioned previously, the still water model is that of a spring-damper, as shown in Fig. 1–3. We describe this elastic stiffness coefficient as the buoyancy force, defined for the beam case as

$$k = \rho_w \, g \, b \tag{1.1}$$

where ρ_w is the water density, g the gravitational force and b the beam width. For the plate we use

$$k = \rho_w \, g \tag{1.2}$$

For the damper foundation, Yang [4] showed that the water damping coefficient has very small values and it depends on the dynamic amplification factor. Within this context, we used the recommended water damping coefficient of 0.5 [kg/m-s].

In order to simplify our foundation model, we further assumed that the ice has a temperature of $-30°$C and the water is at $5°$C. We used the following mechanical properties:

Ice Young's Modulus $\rightarrow$ 3 GPa [9]

Poisson's ratio $\rightarrow$ 0.33 [9]

Ice density $\rightarrow$ 920 kg/m^3 [50]

Water density $\rightarrow$ 1000 kg/m^3 [51]

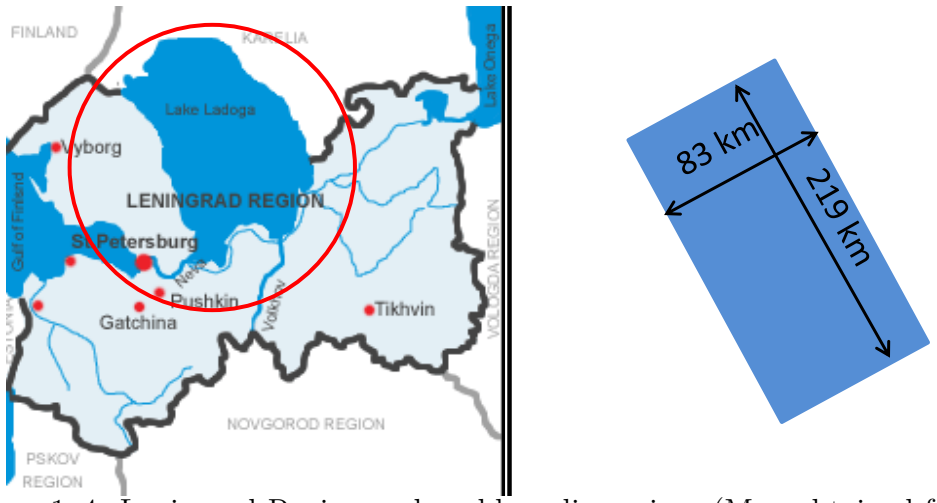

Figure 1–4: Leningrad Region and problem dimensions.(Map obtained from [55])

Figure 1–4 shows that the average dimensions of the Lake Ladoga are about 219 kilometers long and 83 kilometers of width. Research at Baker Lake, Canada [40] demonstrated that the range of the ice thickness lies between 0.0 to 2.5 m, depending of the environmental condition. In addition, Minnesota Department of Natural Resources[1] recommend a minimum of 12 to 15 inches (0.30 m to 0.38 m) of ice thickness for drive a medium truck over a frozen lake. Therefore, we assumed the minimum recommended average thickness of 0.30 meters.

1.2.1 Assumptions

Throughout this work, we made the following assumptions:

1. The velocity of the moving load is constant. We are fully aware that the moving loads may be increasing or decreasing their velocity. However, we assume that the truck enters the ice when it has reached a steady speed. This allows us to ignore the acceleration of the truck. We are fully aware to perform a more complete analysis, we must consider a time-varying load as it moves through the ice; however, our assumption by no means will downplay the results we expect in this work.
2. Beam and plate thicknesses will remain constant through the $x-y$ domain. We know that the ice will have a domain-varying thickness; however, this will add complexity to our analysis because we do not know the actual varying thickness

[1] http://www.dnr.state.mn.us/safety/ice/thickness.html

function, $h(x, y)$. Hence, for sake of simplicity we will assume an average constant thickness throughout the model's domain. We know that for a more complete analysis, we should use some sort of assumed varying thickness function, $h(x, y)$. This inclusion may draw new and very interesting results. However, still the biggest challenge remains that of how to predict the ice varying thickness function.

3. Shear deformation and rotary inertia were neglected through this study. This assumption is very good as the ice-structure has a brittle-like behavior, giving very small room for the shear deformation to act.
4. Ice is considered as isotropic material and the state of stress is that of plane stress, as recommended by Squire et al. [9]. They also recommend that the ice be modeled as an orthotropic material only a greater level of sophistication. Hence, future works could be oriented in how this consideration could affect the presence of resonant regimes.
5. Ice-structural behavior is elastic. Although this behavior can vary for stresses higher than 1 $\mathrm{MN/m^2}$ or if loaded to failure within 2 seconds [45], it will not downplay our confidence in the ice behavior approximation.
6. Young Modulus of Elasticity, E, is assumed constant through all the ice structure. We are fully aware that Young Modulus of Elasticity E depends on porosity and ice temperature [45, 46]. However, this will add complexity to our analysis because we do not know the actual varying porosity and temperature functions. Hence, for sake of simplicity we will assume an average constant Young Modulus of Elasticity throughout the model's domain. Hence, future works could be oriented in how this consideration could affect the presence of resonant regimes.
7. The entire ice-structure is resting over still water. There might be some motion under the water, but such motion may be ignored for lakes.
8. The frozen ice rests completely above the water. We are fully aware that the part of the frozen ice will be submerged. However, we encounter the challenge to know how much of it is really submerged and such analysis would require a three-dimensional model. The scientific community should be aware that our results are

valid only under this assumption because submerging partially the ice most likely will change the results we present in this work.

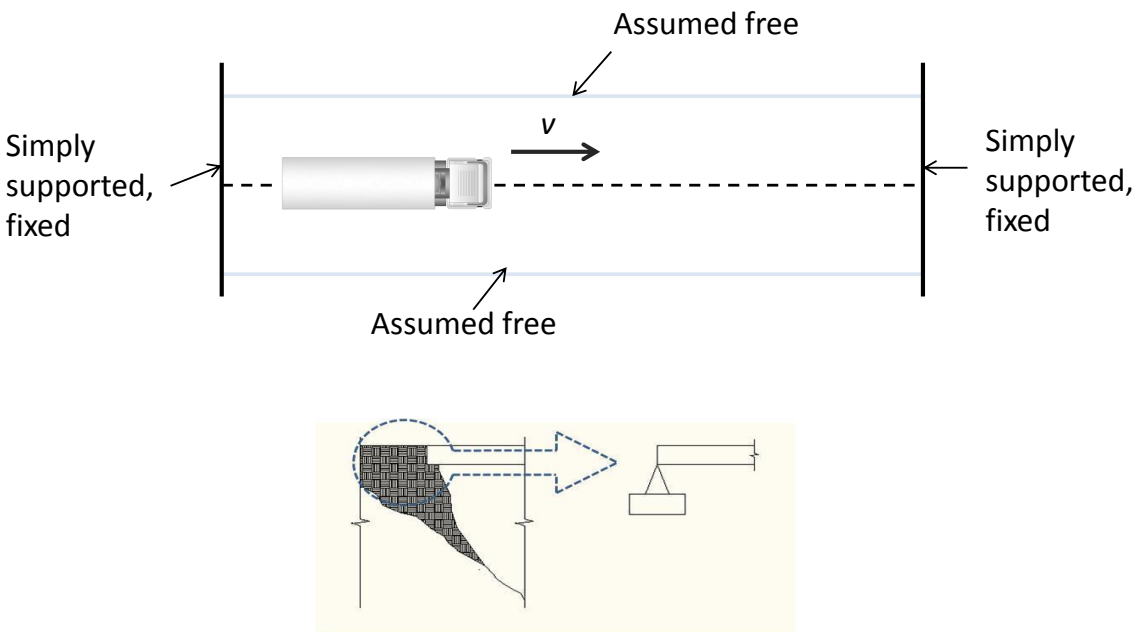

Figure 1–5: Model Boundaries Condition.

9. The modeled boundary conditions for the ice-structure are shown in Fig. 1–6 and can be summarized as follows: simply-supported at $x = 0, L$ and free at $y = 0, b$. At $x = 0, L$ is the location where the trucks enter the ice and they are flushed with the land surface. At first we assumed zero bending moment in order to validate our model against the analytical solution. Once the results were compared, we model using the fixed-fixed boundary conditions. In addition, since the load is applied far from the edges $y = 0, b$ would a good assumption to model it as free. In the finite element model changing these boundary conditions does not add any complexity whereas in the analytical solution it would.
10. Based on the fact that the water is an incompressible fluid, it was assumed that when the ice deflects over the water, the water dissipates far away from the point of action.
11. Interference between deflection fields generated by two trucks results in partial cancelation at about 53 m separation of the maximum the deflection amplitude. Otherwise, this interference is reinforcement at 107 m [41, 42]. In this work it

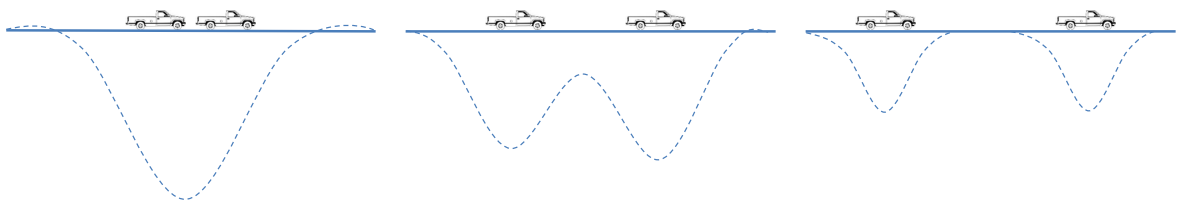

Figure 1–6: From left to right: Increment in deflection amplitude due to interference cancelation, interference due to vehicles approximation and vehicles are separate enough for neglect interference.

was assumed that moving vehicles are separate enough in order to neglect these behaviors. Figure 1–6 shows this phenomenon.

1.3 Goals

1.3.1 Overall Goals

The following statements summarize the goals and scope of this work:

1. Develop a finite element model to predict the unexpected failure behavior of the elastically and viscoelatically ice-structure subject to a constant moving load.
2. Using the finite element analysis, determine the critical velocity for the beam and plate models with an elastic and viscoelastic supported foundations.
3. Using developed finite element model, determine if the weight has any effect on the critical velocity.

1.3.2 Intellectual Merit

To this day, frozen lakes are used as transportation roads, developing the interest to structural engineers and researchers to predict the ice behavior. Using the critical velocity as the resonance trigger may help to safely use lakes as transportation roads. This work presents an approach to determine the critical velocity using the finite element analysis for unexpected ice failure, which the literature shows very little—not to say no—work using a computational approach. In this context, this work may be using as a framework for more complex analyses of structures subject to moving loads at high velocity. In short, there exists very little work, not to say none, that predicts ice-failure using resonance of the moving load; and this work is one-of-its kind as it provides a finite element approach to predict ice unexpected

failure due to moving loads using critical velocity.

1.3.3 Broader Impacts

This work will enrich the field of structural engineering, allowing engineers and/or scientists to learn how critical velocities can be calculated using the Finite Element Method. Also, history will also benefit since we are providing a possible explanation for ice failure at *"Road of life"*. The applications are beyond the frozen lake transportation roads because this project will also contribute to the safety of common structures as bridge and train rails. Special interest exists in military agencies. Recently, McNab et al. [6] presented an overview of the naval railgun development program, in which the authors show the need to reach the long-term Navy goal of 10,000-round lifetime, considering damage that occurs at high velocity. Nechitailo and Lewis [3] stated that the proper use of materials and components as well as optimized barrel geometry should contribute to the longevity of the launchers and to the accuracy of the launched projectiles. This work will also help them as they design safer railguns.

1.4 Approach

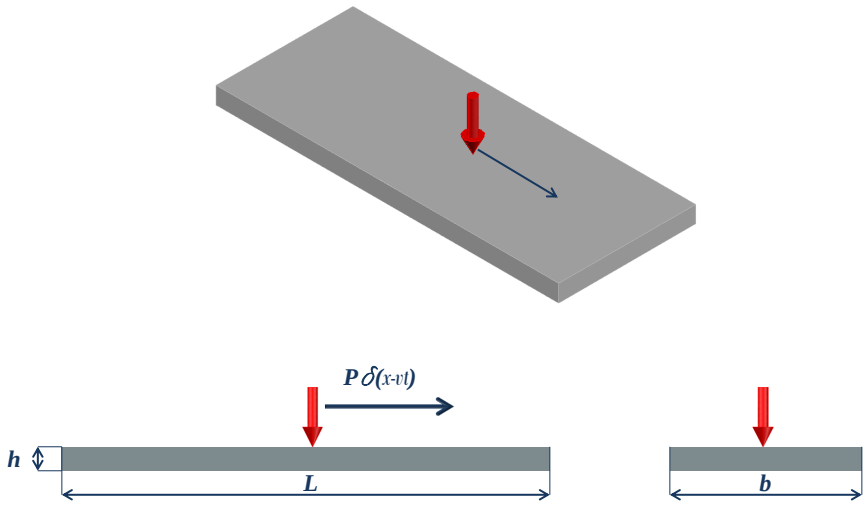

Figure 1–7: Moving load over rectangular structure

The first step in this work consists in modeling the truck-ice-water system as an Euler-Bernoulli beam under elastic and viscoelastic foundations. We plan to conduct the analysis separately, that of elastic and viscoelastic one, in order to analyze the effects of the damping coefficient in the critical velocity. This will help us to identify the change in critical velocity, if any, in the two models. For the studied model, shown in Fig. 1–7, we assumed that the load only moves along the x-axis, the main axis of the beam. We use plan on using the following differential equation of motion [24]:

$$EI\frac{\partial^4 w(x,t)}{\partial x^4} + \rho A\frac{\partial^2 w(x,t)}{\partial t^2} + c\frac{\partial w(x,t)}{\partial t} + kw(x,t) = P\delta(x - vt) \tag{1.3}$$

where w is transverse deflection, x the spatial variable, t the time variable, E the modulus of elasticity, I the second moment of inertia of the beam's cross-section, ρ the mass density of the ice, A the beam cross-sectional area, c the coefficient of viscous damping per unit of length of the water, k the constant representing modulus of the elastic foundation of the water, and P is the force of the moving load at a speed v.

The second step consists in modeling the truck-ice-water system as a kirchhoff Plate under elastic and viscoelastic foundations with loads traveling only in the

x–axis. We use plan on using the following differential equation of motion [39]:

$$D\left[\frac{\partial^4 w(x,y,t)}{\partial x^4}+2\frac{\partial^4 w(x,y,t)}{\partial x^2\partial y^2}+\frac{\partial^4 w(x,y,t)}{\partial y^4}\right]+\cdots$$
$$\cdots+\rho\,h\,\frac{\partial^2 w(x,y,t)}{\partial t^2}+c\,\frac{\partial w(x,y,t)}{\partial t}+k\,w(x,y,t)=P\,\delta(x-vt)\,\delta(y) \tag{1.4}$$

where x and y are the spatial variables, h the plate's thickness, D the flexural rigidity of the plate defined as

$$D=\frac{Eh^3}{12(1-\nu^2)}, \tag{1.5}$$

and ν is the Poison's ratio.

The computational models will consist is developing the weak form of the equations of motion and applying the finite element method in a home-based finite element code developed in MATLAB®. We plan to compare our results for those of plates with elastic foundation available in the literature or develop our own analytical solution. Once we validate our finite element model, then we will proceed to solve our frozen lake subject to moving load problem. At the end, we expect to predict the ice-cracking at Lake Ladoga using critical velocity as a resonance failure.

1.5 Thesis Outline

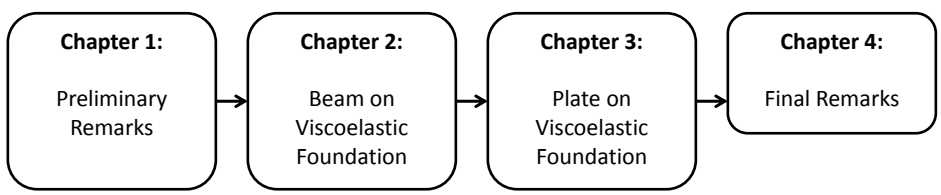

Figure 1–8: Thesis outline.

Figure 1–8 shows the general thesis outline for this work. Through Chapter 1 we intended to provide a general overview of the problem, the motivation, main assumptions, our goals, and how we plan to achieve them. It is not our intention to provide a huge literature survey in this chapter rather to provide the reader an overview of the problem and how we plan to solve the problem. Chapter 2 will address the problem of moving loads on ice-structures modeled using beams over elastic and viscoelastic foundations. This chapter will include the corresponding literature review, computational and analytical models, and the results to the beam

model. Chapter 3 will address the problem of moving loads on ice-structures modeled using plates over elastic and viscoelastic foundations. This chapter will include the corresponding literature review, computational and analytical models, and the results related to the plate model. Lastly, in Chapter 4 we provide our final thoughts by including our conclusions and giving recommendations on how to further expand this work.

CHAPTER 2.
FEA OF UNEXPECTED FAILURE OF LAKE-ICE MODELED AS A VISCOELASTICALLY SUPPORTED BEAM SUBJECTED TO MOVING LOADS AT CRITICAL VELOCITY

The next two chapters enclose the two models for our lake-ice structure. In this chapter we plan on modeling the Lake-ice structure as a beam. Hence, we plan on using the finite element model to predict the unexpected failure of lake-ice when modeled as a viscoelastically supported beam subject to moving loads. The still water on which the ice rests is assumed as a viscoelastic foundation, as previously discussed in Chapter 1. Here, we present the weak form of the equations of motions and a method to predict the unexpected failure of ice-water structures though a novel approach consisting of determining the ice-structure resonance by using the critical velocity. Our model obtained the exact results when compared to the analytical model of steel viscoelastically supported beams subject to moving loads. With this approach, we provide a first possible explanation for the *"Road of life"* at Lake Ladoga phenomena using a beam model.

2.1 Background

In the literature, we find two beam models: (i) beams with elastic foundation, (ii) and beams with viscoelastic foundation. However, very little information is known in terms of ice-behavior when modeled as beam under the above foundations.

2.1.1 Concept of Stability

What we are trying to prove is that the main cause of the unexpected catastrophic lake-ice failure is the loss of stability due to resonance at the critical velocity. Now, buckling is defined as failure due to excessive displacements (loss of structural

stiffness), and/or loss of stability of an equilibrium configuration of the structure [53]. The buckling load is the load at which the current equilibrium state of a structural element, or structure, suddenly changes from stable to unstable, and is, simultaneously, the load at which the equilibrium state suddenly changes from that previously stable configuration to another stable configuration with or without an accompanying large response. Thus, the buckling load is the largest load for which stability of equilibrium of a structural element or structure exists in its original (or previous) equilibrium configuration. Now, when resonance occurs in the structure it also causes loss of stability. Hence, there has to be a velocity that causing the lake-ice structure to act as if it had buckled.

Timoshenko [1] was one of the pioneers to relating a moving load over a structure with the buckling load. He compared the effect of the moving load speed and the beam deflection with an increase of additional compressive force. He stated that the effect of the moving load speed, v, on the deflection is analogous to that of an additional compressive force, S, which may be determined using the following relationship:

$$S = \rho\, A\, v^2 \tag{2.1}$$

where ρ is the density of the structure, A the cross-sectional area and v the speed of the moving load. Timoshenko [1] has also stated that in the case of a long beam resting on an elastic foundation subjected to a gradually increasing longitudinal force, S, the beam becomes unstable due to loss of its structural stiffness, enforcing the presence of beam buckling. This phenomena occurs when the critical value of compressive force becomes

$$S_{cr} = 2\sqrt{E\, I\, k} \tag{2.2}$$

where S_{cr} is the critical compressive force, E the elastic modulus, I the beams's cross-sectional moment of inertia, and k the elastic foundation constant. Now, combining Eqs. 2.1 and 2.2, we can obtain an expression for the critical value of the load speed, where the structure losses its structural stiffness, and defined it as

follows [1]:

$$v_{cr}^2 \rho A = 2\sqrt{E\,I\,k} \quad \rightarrow \quad v_{cr} = \sqrt{\frac{2\sqrt{E\,I\,k}}{\rho A}} \tag{2.3}$$

The velocity of the moving load has an effect on the wave propagation [2, 25]. Kenney [2] presented a time invariant solution to Eq. 1.3 and Seong-Min et al. [25] studied its dynamic response. Both studies showed that when the moving load has lower speeds, the solution approaches to the static solution, decreases exponentially with the distance from the load, that the solution is localized. In order words, the deflected shape is symmetric with respect to the vertical axis, which passes through the center of the load. As velocity increases, more pronounced fluctuations occur and the deflected region is even more widely spread. In other hand, for speeds greater than "critical speed", the responses behind and ahead of the load are very different. The frequency of the fluctuations in front of the load is larger than the ones behind the load, and the amplitudes of the fluctuations in front of the load are smaller than ones behind the load. As the velocity increases, the amplitudes of the fluctuations in front of the load decrease significantly. The frequency of the fluctuations in front of the load increases with an increase in velocity while corresponding frequency behind the load decreases.

Seong-Min et al. [25] also studied the effect of the loaded length and a moving harmonic load. They showed that as the loaded length increases, the maximum displacement decreases, but the critical velocities occur at almost the same value. Also, the distance lag between the maximum amplitude point and the center of the load increases proportionally with the load length. For larger load lengths, the distance lag increases with increasing velocity until it approaches the critical velocity. Near the critical velocity it suddenly drops to a negative value but then it increases again.

2.1.2 Elastically Supported Beam

We may study elastically supported beams subject to moving loads using either Euler-Bernoulli or Timoshenko beam models. As previously stated, we plan to us the Euler-Bernoulli Beam Theory. Timoshenko [1], Kenney [2] and Nechitailo and

Lewis [3] showed that the vibration induced by a moving load on a structure may increase its dynamic deflection and stresses when compared with its static state. The equation of motion for a viscoelastically supported beam is:

$$EI\,\frac{\partial^4 w(x,t)}{\partial x^4} + \rho A\,\frac{\partial^2 w(x,t)}{\partial t^2} + c\,\frac{\partial w(x,t)}{\partial t} + k\,w(x,t) = P\delta(x - vt) \tag{2.4}$$

The Timoshenko beam model, which takes into account shear deformation and rotational inertia effects, may also be used to study the effects of a moving load on elastically supported beams [7]. As compared to the Euler-Bernoulli beam model suggesting one critical velocity, the Timoshenko beam model produced total of three critical velocities. Also the displacements, rotation and bending moments increase in an unbounded manner when the load speed approached these critical velocities.

Nechitailo et al. [3] compared the results obtained from a finite element software, for load speeds near the shear wave and longitudinal wave speeds in hypervelocity launchers rails. The results did not reveal any resonance at these values, demonstrating that the lower critical velocity stated by Timoshenko are the only significant in terms of beam deflection.

Although various authors [1–3, 5, 7–15, 24–26], have contributed to the study of moving loads on elastically supported beams, especially in the transportation area, very little work has been presented regarding the study of the effect of moving loads on unexpected failure of lake-ice structures when elastically supported using finite element analysis and its influence in the loss of beam's stability at the critical velocity.

2.1.3 Viscoelastically Supported Beam

Kenney [2], Seong-Min et al. [25] and Achenbeck et al. [11] incorporated damping in their respective works. They all concluded that an increase in the damping ratio, results in a significant reduction of the beam's maximum amplitude and bending moment. Furthermore, Seong-Min et al. [25] showed that when we analyze the resulting mode shapes, the damping turns the deflected shape into a not too long but a symmetric one, creating a lag between the maximum amplitude point and the

center of the load. They also stated, that the damping ratio has no effect on the critical frequency.

Finite element analysis had been used for the modeling of moving loads over different viscoelastic foundations. As an example, Andersen et al. [26] modeled an infinite Euler beam over a linear elastic Kelvin foundation with linear viscous damping. They demonstrated how useful the finite element models are for obtaining results were no analytical solutions can be found. But similar to the case of elastic foundation, the most of the work exists in the transportation area [16–22]. However, very little work has been presented regarding the study of the effect of moving loads on unexpected failure of lake-ice structures when viscoelastically supported using finite element analysis and its influence in the loss of beam's stability at the critical velocity.

2.2 Computational model

As we previously mentioned, the main goal of this work is try to solve the phenomena around the *"Road of life"* at Lake Ladoga. Here, we will use the critical velocity as the basis to try to solve this problem. We will do so by modeling the ice-structure as an elastic and viscoelastically supported Euler-Bernoulli beam.

2.2.1 Elastically Supported Beam: Analytical

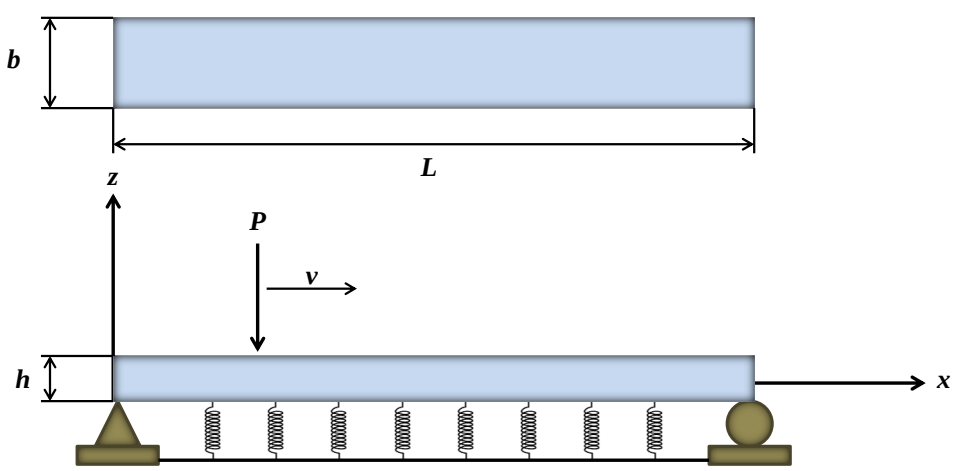

Figure 2–1: Simply supported beam over elastic foundation with moving load.

First, we will deal with the analytical solution and then develop the finite element model. Analytical solutions for beams has been developed by various researchers [1–3, 13, 14, 24]; however, we will use the solution presented by Mallik et al. [5] for infinite beams. Although our lake is not an infinite one, the line of motion of the truck is very long and it may be considered long enough to approximate it as infinite. We will later show that the results for beam with a ratio less than $b/L = 0.379$ give the same critical velocity.

The behavior of a undamped elastically supported beam under the effect of moving loads, as shown in Fig. 2–1, is defined by

$$EI\,\frac{\partial^4 w(x,t)}{\partial x^4} + \rho\,A\,\frac{\partial^2 w(x,t)}{\partial t^2} + k\,w(x,t) = P\,\delta(x - vt) \tag{2.5}$$

Let us rearrange the above equation and introduce the following two new constants: $n^2 = k/EI$ and $m = \rho A/2EI$. This leads us to the following equation

$$\frac{\partial^4 w(x,t)}{\partial x^4} + 2\,m\,\frac{\partial^2 w(x,t)}{\partial t^2} + n^2\,w(x,t) = \frac{P\,\delta(x - vt)}{EI} \tag{2.6}$$

We can show that the solution to the transverse deflection to Eq. 2.6, is:

$$w(x,t) = \int_{-\infty}^{\infty} w^*(\gamma,t)e^{-i\gamma x}d\gamma \tag{2.7}$$

where

$$w^* = \int_{-\infty}^{\infty} w(x,t)e^{-i\gamma x}dx \tag{2.8}$$

and Equations 2.7 and 2.8 constitute a Fourier transformation pair. Now, we multiply both sides of Eq. 2.6 by $e^{-i\gamma x}$ and integrating by parts over x from $-\infty$ to $+\infty$, and assuming that in w its space derivatives vanish at $x = \pm\infty$, to get the following expression:

$$\gamma^4 w^* + n^2 w^* + 2m\frac{d^2 w^*}{dt^2} = \frac{P}{EI}e^{-i\gamma vt} \tag{2.9}$$

Now, substitute $w^* = W^* e^{-i\gamma vt}$ in Eq. 2.9 to get

$$(\gamma^4 + n^2 - 2\,m\,v\gamma^2\,v^2)W^* = \frac{P}{EI} \tag{2.10}$$

Now, we use Eq. 2.7 to get

$$\begin{aligned} w(x,t) &= \frac{P}{EI}\frac{1}{2\pi}\int_{-\infty}^{\infty}\frac{e^{i\gamma(x-vt)}}{\gamma^4-2mv^2\gamma^2+n^2}d\gamma \\ &= \left(\frac{P}{EI}\right)\left(\frac{1}{2\pi}\right)2\pi i\sum \mathrm{R}, \end{aligned} \tag{2.11}$$

where R are the residues at four simple poles γ_1 to γ_4 given in Appendix A (Mallik et al. [5]). Once we get our residues, the solution to Eq. 2.5, for $\xi > 0$, where $\xi = x - vt$, is defined by

$$w(x,t) = \frac{Pe^{-M\xi}}{4EInMN}[N\cos N\xi + M\sin N\xi], \tag{2.12}$$

where for convenience we introduce $M = \frac{n-mv^2}{2}$ and $N = \frac{n+mv^2}{2}$. Similarly, for $\xi < 0$ the solution is defined as

$$w(x,t) = \frac{Pe^{\alpha\xi}}{4\,EI\,m\,M\,N}[N\cos N\xi - M\sin N\xi] \tag{2.13}$$

Equations 2.12 and 2.13 show that when $M = 0$, the division by zero results that the deflection of the beam shoot up to infinity. It can be noticed that $M = 0$ occurs when $v = n/m$, which is called the critical parameter. Rearranging v in term of the original system parameters results in the following equation:

$$v_{cr} = \sqrt{\frac{2\sqrt{EIk}}{\rho A}} = \sqrt[4]{\frac{E\,g\,h}{3\,\rho}} \tag{2.14}$$

which matching that obtained by Timoshenko's expression for critical velocity, Eq. 2.3. Thus, at the critical velocity, the beam's deflection reaches its maximum value, which will be the basis of the proposed formulations.

2.2.2 Elastically Supported Beam: FEA

In order to create a FE-based solution to Eq. 2.5, we will start by developing the weak formulation. Let us multiply Eq. 2.5 with a test function ϑ and integrate over the domain [54]. Note that the formulation is developed for one arbitrary element, being this the reason to use local coordinates $0 < \bar{x} < \ell_e$. Here ℓ_e is the length of

the beam element as shown in Fig. 2–2. This leads to

$$\int_0^{\ell_e} \vartheta \left[EI \frac{\partial^4 w(\bar{x},t)}{\partial \bar{x}^4} + \rho A \frac{\partial^2 w(\bar{x},t)}{\partial t^2} + k\, w(\bar{x},t) - P\, \delta(\bar{x} - vt) \right] d\bar{x} \tag{2.15}$$

After integrating by parts and applying the corresponding boundary conditions, we get[1]

$$\int_0^{\ell_e} \left(EI \frac{\partial^2 \vartheta}{\partial \bar{x}^2} \frac{\partial^2 w}{\partial \bar{x}^2} + \rho A\, \vartheta \frac{\partial^2 w}{\partial t^2} + k\, \vartheta\, w - P\, \vartheta \right) d\bar{x} \tag{2.16}$$

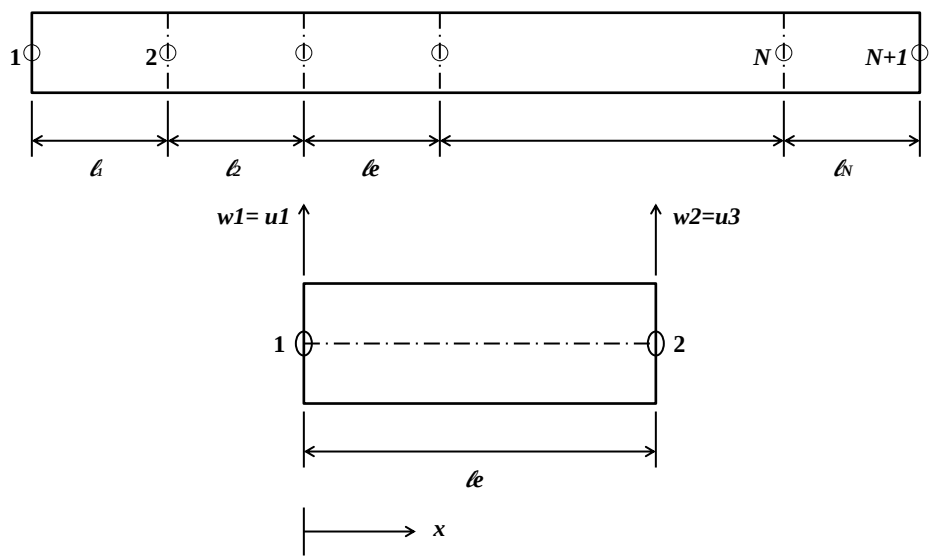

Figure 2–2: Discretization of a beam elements.

Now, we proceed to continue to discretize the beam's domain as shown in Fig. 2–2. For the time dependent problems, we use a semidiscrete formulation which involves approximation of the spatial variation of the dependent variable. The discretization of Eq. 2.16 leads to

$$w(\bar{x}, t_s) = \sum_{j=1}^{n} u_j^e(t_s)\phi_j^e(\bar{x}) = \sum_{j=1}^{n} (u_j^s)^e \phi_j^e(\bar{x}) (s = 1, 2, ...) \tag{2.17}$$

[1] Note that for now we will write $P\delta(x - vt)$ as P. We will deal with the moving load later in Section 2.2.4.

where $(u_j^s)^e$ is the value of $u(\bar{x}, t)$ at time $t = t_s$ and at node j of the element e. Let us choose the test function as the shape function, $\vartheta = \phi_i(x)$, and substitute Eq. 2.17 into Eq. 2.16, to obtain

$$0 = \int_0^{\ell_e} \left\{ EI \frac{d^2\phi_i}{d\bar{x}^2} \left(\sum_{j=1}^{n} u_j \frac{d^2\phi_j}{d\bar{x}^2} \right) + \rho A \, \phi_i \left(\sum_{j=1}^{n} \frac{d^2 u_j}{dt^2} \phi_j \right) + \cdots \right.$$
$$\left. \cdots + k \, \phi_i \left(\sum_{j=1}^{n} u_j \phi_j \right) - \phi_i P \right\} d\bar{x} \tag{2.18}$$

For simplicity, we may write the above equation may in its matrix form

$$[K]u + [M]\ddot{u} = \{F\} \tag{2.19}$$

where

$$\begin{aligned} [K] &= \int_0^{\ell_e} \left\{ EI \frac{d^2\phi_i}{d\bar{x}^2} \frac{d^2\phi_j}{d\bar{x}^2} + k\phi_i\phi_j \right\} d\bar{x} \\ [M] &= \int_0^{\ell_e} \rho A \phi_i \phi_j \, d\bar{x} \\ \{F\} &= \int_0^{\ell_e} \phi_i P \, d\bar{x} \end{aligned} \tag{2.20}$$

2.2.3 Viscoelastically Supported Beam: FEA

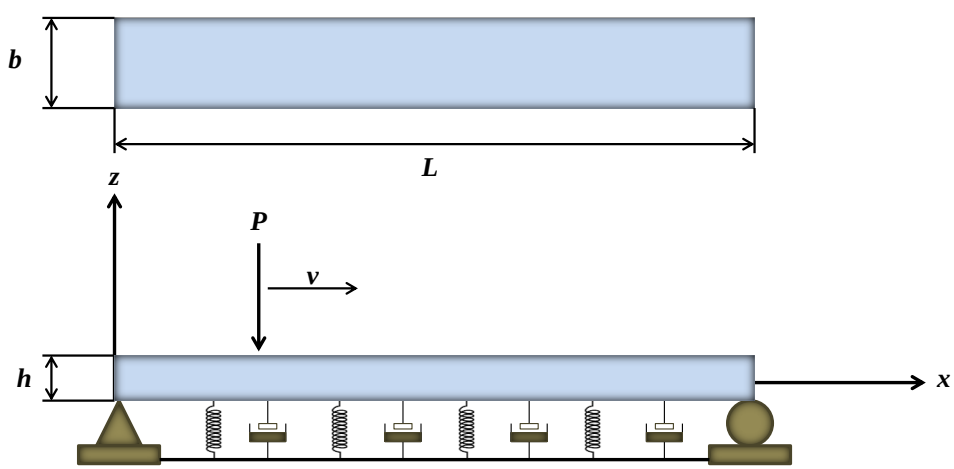

Figure 2–3: Simply supported beam over viscoelastic foundation with moving load.

Now, we formulate the finite element beam model for a viscoelastic foundation, as shown in Fig. 2–3. The main difference is that now we include the damping coefficient to the previous model. This viscosity is not of the lake-ice structure but

of the still water acting on the beam. The following equation of motion describes this scenario:

$$EI\frac{\partial^4 w(\bar{x},t)}{\partial \bar{x}^4} + \rho A\frac{\partial^2 w(\bar{x},t)}{\partial t^2} + c\frac{\partial w(\bar{x},t)}{\partial t} + kw(\bar{x},t) = P \tag{2.21}$$

We use a similar procedure as for the case of elastically supported beam, by formulating the differential equation into its weak formulation and later the discretizing it. Equation 2.21 is multiplied by the test function ϑ and after integration by parts and applying the corresponding boundary conditions, the weak form is obtained as follows:

$$\begin{aligned} 0 = \int_0^{\ell_e} \Big\{ EI\,\frac{\partial^2 \vartheta}{\partial \bar{x}^2}\frac{\partial^2 w}{\partial \bar{x}^2} + \rho A\,\vartheta\frac{\partial^2 w}{\partial t^2} + c\,\vartheta\frac{\partial w}{\partial t} + \cdots \\ \cdots + k\,\vartheta w - P\,\vartheta \Big\}\, d\bar{x} \end{aligned} \tag{2.22}$$

Substituting the displacement approximation given in Eq. 2.17 into Eq. 2.22 we get,

$$\begin{aligned} 0 = \int_0^{\ell_e} \Bigg[EI\frac{d^2\phi_i}{d\bar{x}^2}\left(\sum_{j=1}^{n} u_j \frac{d^2\phi_j}{d\bar{x}^2}\right) + \rho A\phi_i\left(\sum_{j=1}^{n}\frac{d^2 u_j}{dt^2}\phi_j\right) + \cdots \\ \cdots + c\phi_i\left(\sum_{j=1}^{n}\frac{du_j}{dt}\phi_j\right) + k\phi_i\left(\sum_{j=1}^{n} u_j\phi_j\right) - \phi_i P \Bigg]\, d\bar{x} \end{aligned} \tag{2.23}$$

For simplicity, we will write the above equation in its matrix form

$$[M]\ddot{u} + [C]\dot{u} + [K]u = \{F\} \tag{2.24}$$

where the damping matrix is defined by

$$[C] = \int_0^{\ell_e} c\phi_i\phi_j\, d\bar{x} \tag{2.25}$$

2.2.4 1D Moving Finite Element Method

Now, we will explain how we dealt with the moving load. For this we plan on using Figs. 2–4 and 2–5 for this discussion. We will call the approach used here as the moving finite element (MFE) method. The MFE method treats the moving load as a moving part of the entire system, so that the transverse inertial effects caused by the moving mass may easily be taken into account [47]. When a beam is subjected to a concentrated force P, the forces on all the nodes of the beam are equal to zero except the nodes of element e that are subjected to the concentrated force. Therefore, the force vector takes the following form [48]:

$$\{F\} = \{0\,0\,0 \cdots F_1^e(t)\, F_2^e(t)\, F_3^e(t)\, F_4^e(t) \cdots 0\,0\,0\} \tag{2.26}$$

where F_i^e (for $i = 1, \ldots, 4$) represents the equivalent nodal forces of the element e where the force is applied,

$$\{F^e(t)\} = \{F_1^e(t)\, F_2^e(t)\, F_3^e(t)\, F_4^e(t)\}^{\mathrm{T}} = P\{\phi\} \tag{2.27}$$

and $\phi_i(x)$ (for $i = 1, \ldots, 4$) represents the shape functions.

Fig. 2–4 shows the element and node of the beam that are subjected to the concentrated force that cannot be zero. Here, ℓ_e is the length of the element and x the distance along the element to the point of application of P. We defined Δt as the time interval for our model. This time interval is divided in t_{st} time steps. Therefore the total time is defined as:

$$t_{total} = t_{st}\Delta t \tag{2.28}$$

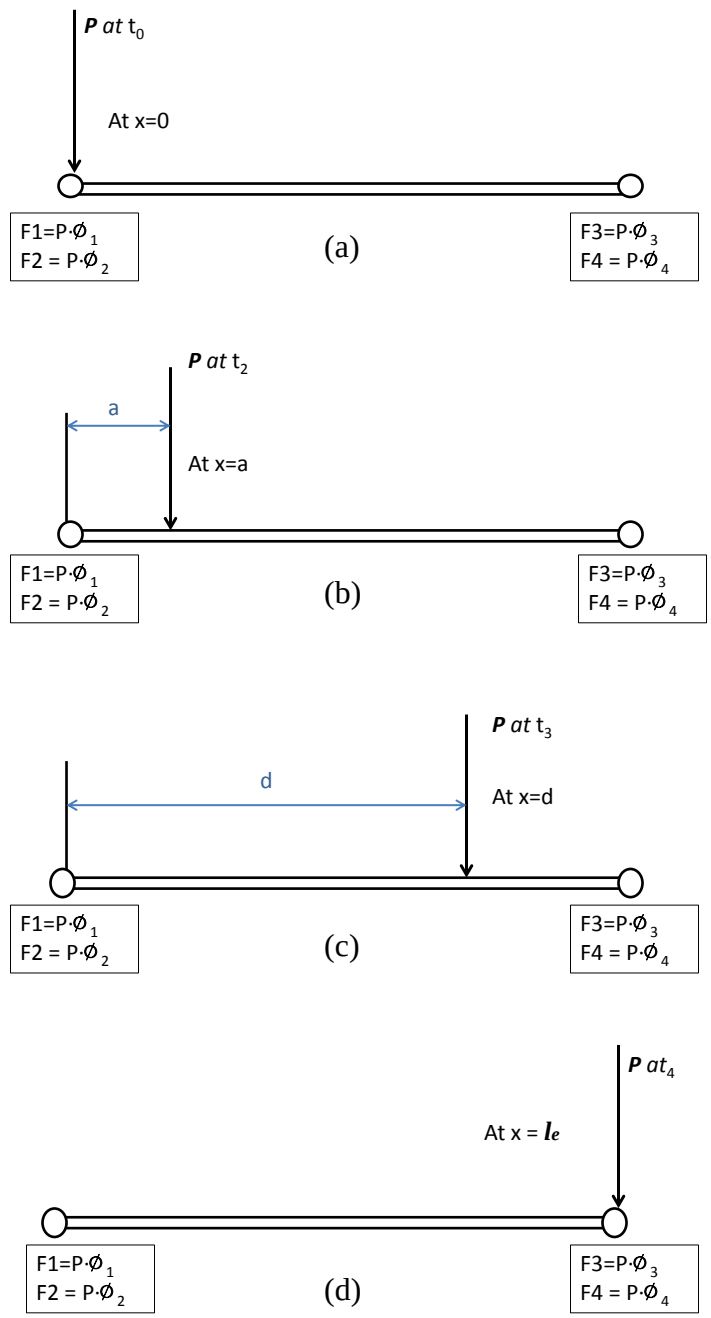

Figure 2–4: The equivalent forces of the element e subjected to a moving load P.

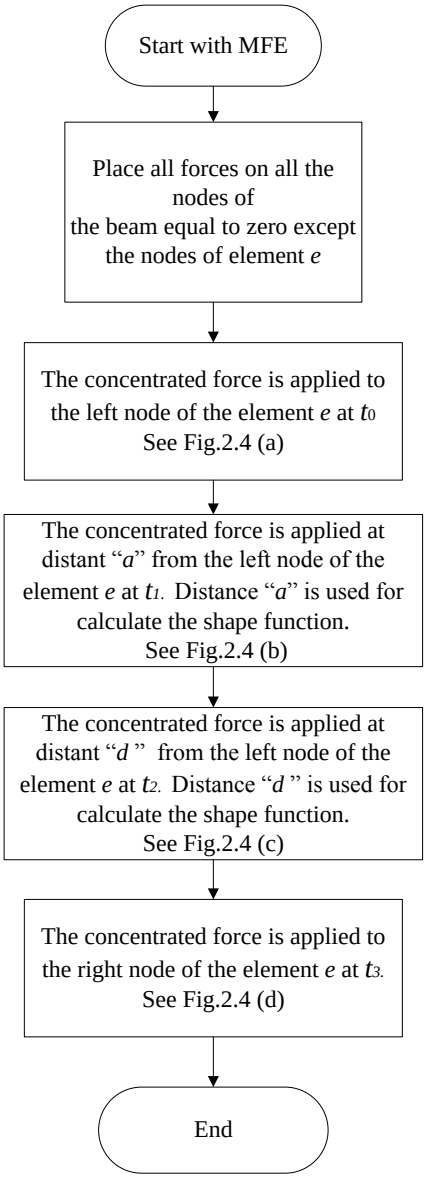

Figure 2–5: Moving Finite Element approach for a single element e.

In Fig 2–4 (a), the concentrated force is applied just over the left node of the element ℓ_e. Then, for the following time step t_{st}, the load is applied at distance a from the left node of the element ℓ_e, as shown in Fig 2–4 (b). This position of the load at any time $t = r\Delta t$ (where r goes from 1 to t_{st}) is given by

$$x_p = Vr\Delta t \tag{2.29}$$

and the element e where the moving concentrated force is applied at any time t can be know from

$$e = \left(\text{The integer part of } \frac{x_p(t)}{\ell_e}\right) + 1 \tag{2.30}$$

Thus, the shape functions $\phi_i(x)$ are written in term of this local distance. Thus the shape functions are redefined as $\phi_i(\varsigma)$, making the shape functions depending of ς instead of x, where ς is defined as

$$\varsigma = \frac{x_p(t) - (e-1)\ell_e}{\ell_e} \tag{2.31}$$

where ℓ_e is the length of the beam element. It should be noted that when ς is an integer, there is only one nodal force, as we would expect, since an integer value for ς means that P is coincident with a node [48].

2.2.5 Newmark Time Integration Scheme

In order to obtain the dynamic response of the force vibration created by the moving load, we used the well-known Newmark time integration scheme. The Newmark integration method is based on the assumption that the acceleration varies linearly between two instants of time. Figure 2–6 outlines the procedure.

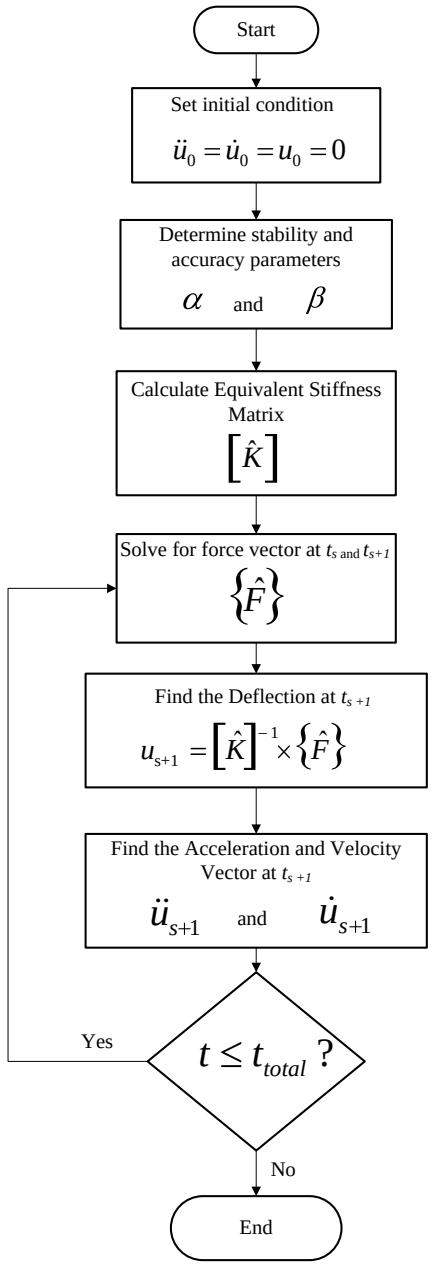

Figure 2–6: Newmark integration scheme flowchart.

The matrix form of our weakened equations of motions, takes the following form:

$$[\hat{K}]_{s+1}\{u\}_{s+1} = \{\hat{F}\}_{s,s+1} \tag{2.32}$$

where

$$\begin{aligned}
\left[\hat{K}\right]_{s+1} &= [K]_{s+1} + a_0[M]_{s+1} + a_1[C]_{s+1} \\
\{\hat{F}\}_{s,s+1} &= \{F\}_{s+1} + [M]_{s+1}(a_0\{u\}_s + a_2\{\dot{u}\}_s + a_3\{\ddot{u}\}_s)\cdots \\
&\qquad \cdots + [C]_{s+1}(a_1\{u\}_s + a_4\{\dot{u}\}_s + a_5\{\ddot{u}\}_s) \\
\{\ddot{u}\}_{s+1} &= a_0(\{u\}_{s+1} - \{u\}_s) - a_2\{\dot{u}\} - a_3\{\ddot{u}_s\} \\
\{\dot{u}\}_{s+1} &= \{\dot{u}\}_s + a_6\{\ddot{u}\}_s + a_7\{\ddot{u}_{s+1}\}
\end{aligned} \tag{2.33}$$

where

$$\begin{aligned}
&a_0 = \frac{2}{\Delta t^2}, && a_1 = \frac{\alpha}{\beta\Delta t}, && a_2 = \frac{1}{\beta\Delta t}, \\
&a_3 = \frac{1}{2\beta} - 1, && a_4 = \frac{\alpha}{\beta - 1}, && a_5 = \frac{\Delta t}{2}\left(\frac{\alpha}{\beta} - 2\right), \\
&a_6 = (1-\alpha)\Delta t, && a_7 = \alpha\Delta t
\end{aligned}$$

Here α and β are the parameters that determine the stability and accuracy of the scheme (Reddy [49]). Note that the calculation of $[\hat{K}]$ and $\{\hat{F}\}$ requires the knowledge of the initial conditions $\{u\}_0$, $\{\dot{u}\}_0$ and $\{\ddot{u}\}_0$. For this work, since the moving load begins on the left support, $\{u\}_0$, $\{\dot{u}\}_0$ and $\{\ddot{u}\}_0$ are zero.

2.3 Results and Discussions

2.3.1 Model Validation

For purpose of validating our model, we used the work by Nechitailo and Lewis [3]. The only difference between the two models was that they used a pressure load and we found an equivalent point load. Their maximum static deflection at the center of the beam resulted in 1.615 mm. In order to find an equivalent point load which results in the same static deflection, we used the analytical solution presented by Hetényi [52] for hinged beams with a load at the center and solved for the equivalent point load:

$$w_{st} = \frac{P\lambda}{2k}\frac{\sinh \lambda L - \sin \lambda L}{\cosh \lambda L + \cos \lambda L} = 1.615 \text{ mm} \tag{2.34}$$

where $\lambda = \sqrt[4]{\frac{k}{4EI}}$. Thus, solving for P we get $P = 449,839$ N. The results are shown in Fig. 2–7 .

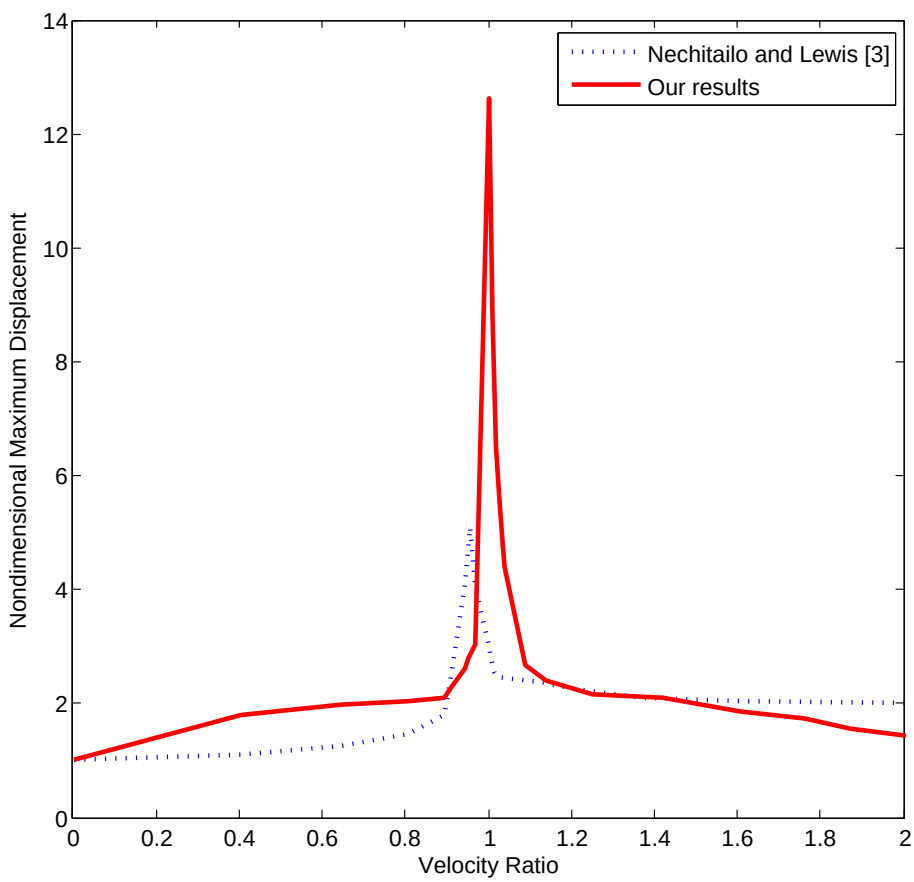

Figure 2–7: Comparison between Nechitailo and Lewis [3] and our model.

Nechitailo and Lewis [3] studied the dynamic behavior of a rail in hypervelocity electromagnetic launchers due to a projectile motion using a finite element software. The calculated analytical critical velocity, based on Timoshenko's equation, was of 1240 m/s. Their results showed a dimensionless deflection, defined as the ratio of peak deflection to static deflection, of 5 at 1185 m/s, that is 95.6% of the rail's critical velocity. As we can see from Fig. 2–7, our model better captured the phenomena occurring at the critical velocity, that of reaching an infinite value for the dynamic amplification. In our model, we got a dynamic amplification factor of 12.6 at 1240 m/s as predicted by Timoshenko's equation; hence, we obtained the exact solution from a theoretical perspective. Also, from Eq. 2.12 and Eq. 2.13 we see that when the load reaches its critical value the deflections shoot up to infinity. This explains why our model gives a dynamic amplication factor higher by 2.5 than the one obtained by Nechitailo and Lewis [3]. This validates our model and we proceeded to model the truck-ice-water structure.

2.3.2 Relationship of the Critical Velocity vs. Width-to-Length Ratio

To solve the problem with the full dimensions it would be an extensive computational effort and perhaps unnecessary, as we explain in the next couple of lines. For this, we studied the effect of various width-to-length beam ratios on the critical. Figure 2–8 shows that for a beam ratio of $b/L < 0.4$, we obtain the same critical velocity. In our case, $b/L = 83/219 = 0.379$ which is less than 0.4 and thus as far as we keep the same ratio the results should be the same. Thus, we used the following values: $L = 1, b = 0.379, h = 1.370 \times 10^{-6}$.

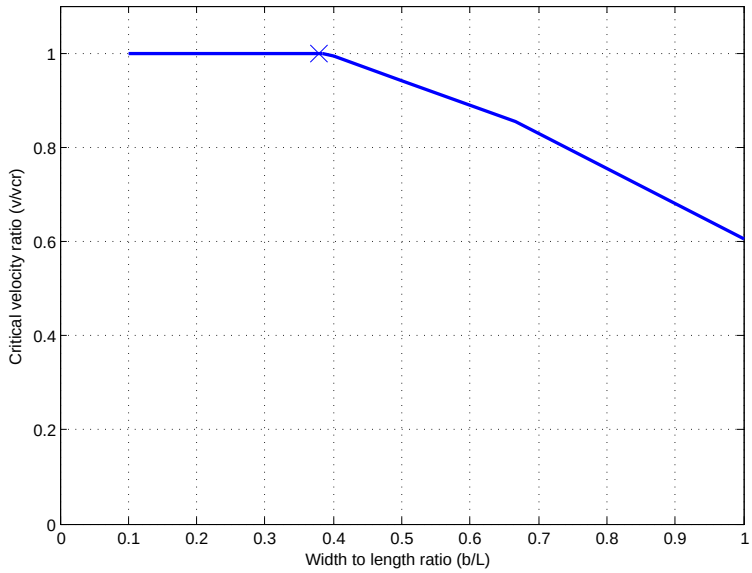

Figure 2–8: Critical velocity with respect to width-to-length ratio.

2.3.3 Convergence Plot

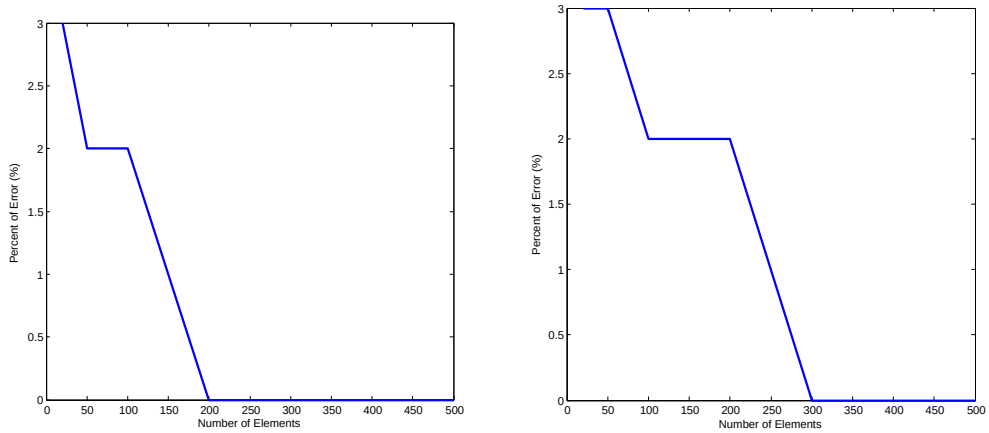

Figure 2–9: Finite element convergence plot for the critical velocity for the elastically supported beam (left) and viscoelastically supported beam (right).

Figure 2–9 shows that when using 200 elements we reach convergence for the elastically supported lake-ice and 300 elements for the viscoelastically supported lake-ice. Hence, there is no need to use any finer mesh than that of 300 elements. We ran all our analysis using 400 elements to ensure convergence throughout our analysis.

2.3.4 Effect of the Elastic Foundation on the Critical Velocity

When the truck-ice-water structure is modeled, our results demonstrated that the transition from the quasi-static regime to a resonant regime occurs gradually, instead of dramatic transition as predicted by Nechitailo and Lewis [3]. This is as a result of a low elastic foundation coefficient presented by the water's buoyancy force, showing that the resonant regimes presence depends also on the foundation properties. Figure 2–10 shows the dynamic amplification for three different elastic foundations. Results show that a higher elastic foundation will produce a smaller nondimensional maximum deflection and greater critical velocity, which is expected.

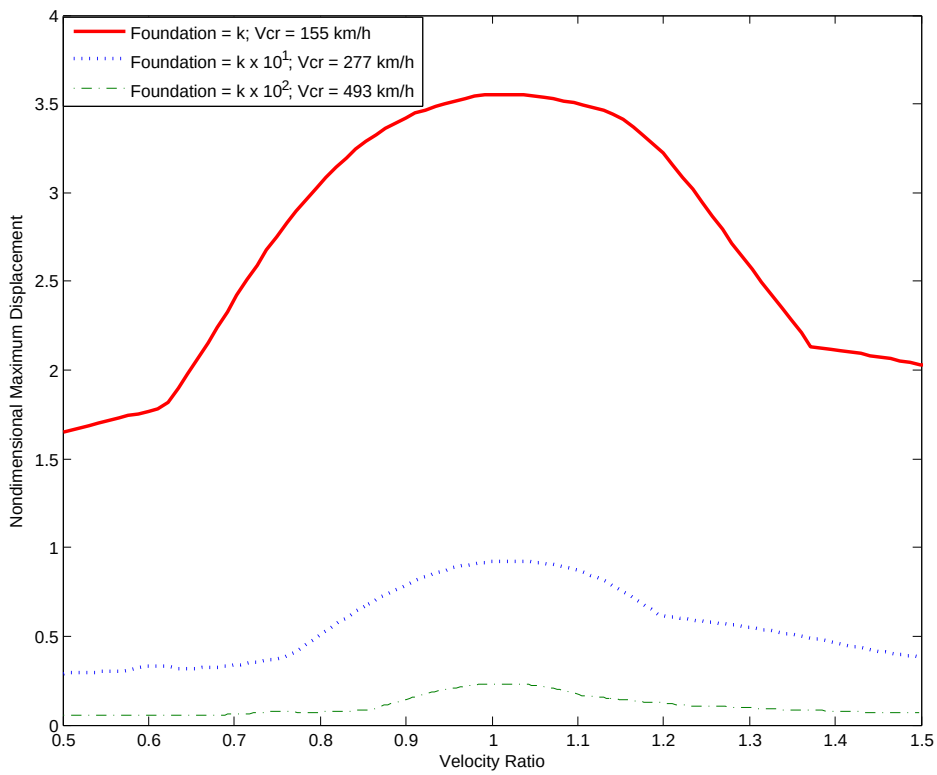

Figure 2–10: Beam's maximum lake-ice deflection with different foundation.

2.3.5 Effect of Damping on the Critical Velocity

Now, we proceed to analyze the effect of the viscoelastic foundation on the critical velocity. The big question was if a change in the damping coefficient would cause any change in the prediction of the critical velocity and maximum nondimensional deflection (actual deflection/static deflection). Figure 2–11 shows that when damping is included, the influence on the predicted critical velocity and maximum

nondimensional deflection is very little. Similar behavior was observed by Nechitailo and Lewis [3], Kenney [2] and Seong-Min et al. [25]. Hence, a water damping factor of 0.5 is very small to mitigate large amplitudes and resonance effects of the moving load over ice.

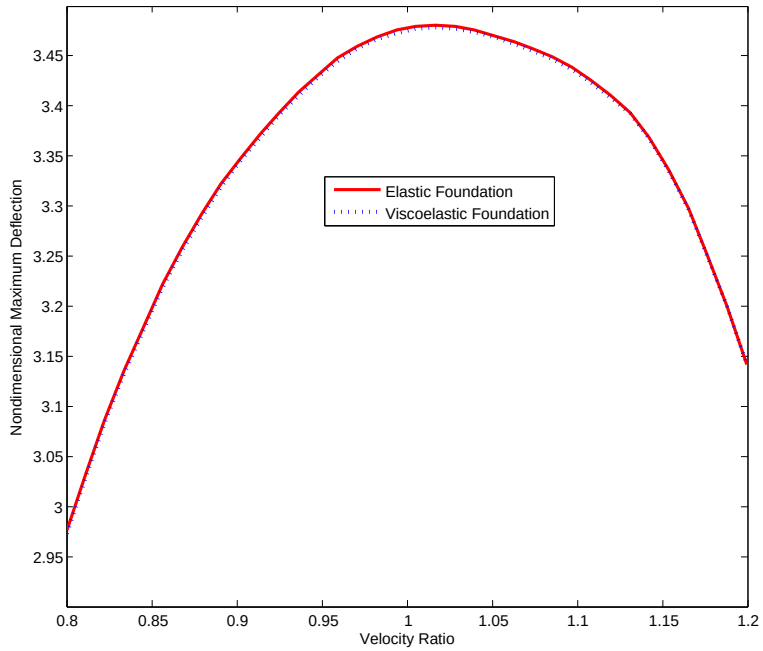

Figure 2–11: Maximum nodimensional beam deflection of lake-ice when water was modeled as an elastic and viscoelastic foundation.

2.3.6 Maximum Beam Deflection Analysis at the Critical Velocity

Now we intend to explain the behavior of the mode shape as the load moving through the Lake-ice structure. Figure 2–12 shows the mode shape obtained when the load travels at three different velocities: half the critical velocity, critical velocity, and twice the critical velocity. As we can see, for velocities less than critical velocity, the beam's shape is similar to that of the static case where the maximum displacement is obtained where the load is located, which is expected since no resonance has occurred. When the velocity approaches its critical value, the frequency of fluctuations in front of the load increases compared with the fluctuations behind the load, showing a "resonance-effect". As the velocity continues increasing above the critical velocity, the frequency of the fluctuations in front of the load increases as well, and the amplitudes of the fluctuations in front of the load are smaller than

those behind the load. This shows that indeed there is a resonance-effect at the critical velocity.

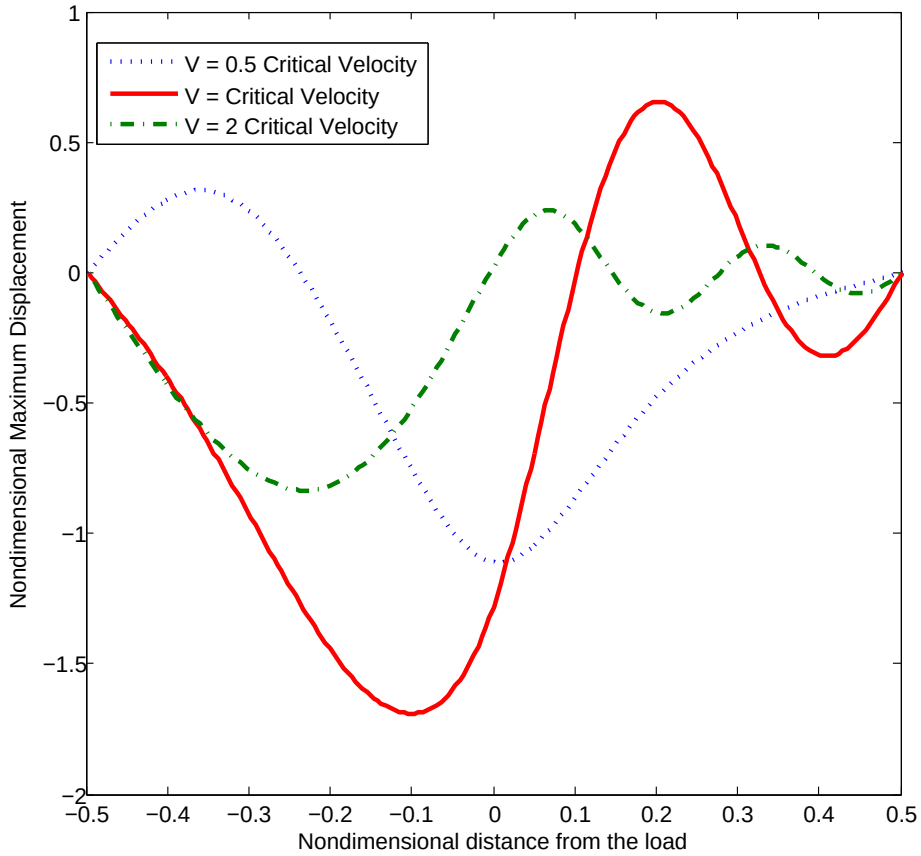

Figure 2–12: Beam mode shapes at different critical velocity ratio.

2.3.7 Effect of Different Boundary Conditions on the Critical Velocity

We modeled our lake-ice structure using a simply-supported boundary condition. However, as discussed in Chapter 1, the most-realistic boundary conditions for our problem should be fixed-fixed. Figure 2–13 shows the comparison between the simply-supported and fixed-fixed boundary conditions. We see that the maximum nodimensional deflection for simply-supported occurs at about 155 km/h and for fixed-fixed occurs at 159 km/h which is a 3% difference. Also, we can observe that for the fixed-fixed boundary condition the structure reached 84% of the maximum deflection reached per simply supported, which is expected. Hence, when modeling the Lake-ice as a beam, either boundary condition will produce the resonance effect for roughly the same critical velocity.

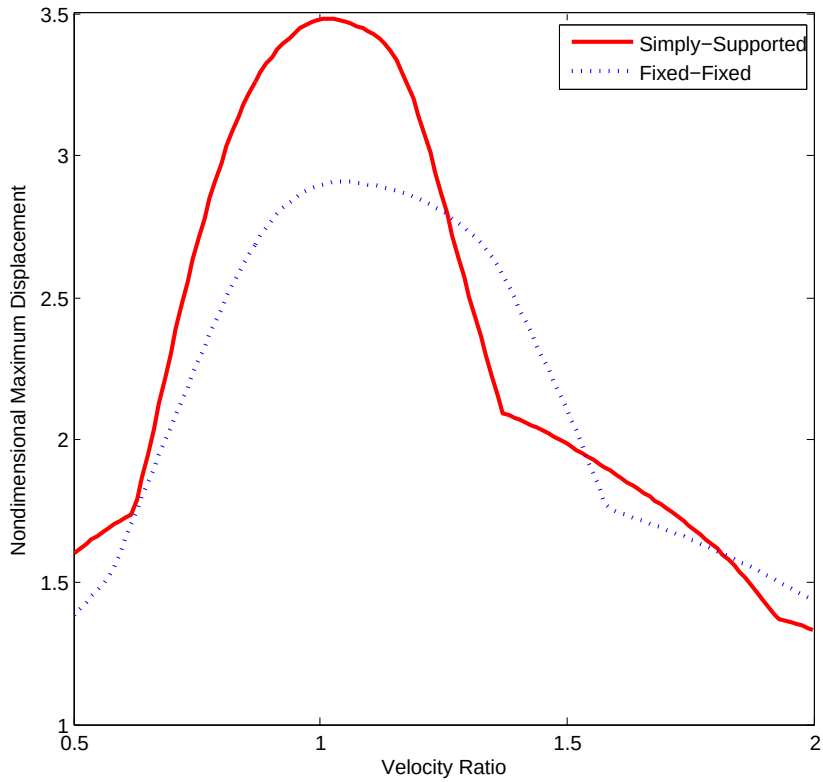

Figure 2–13: Maximum nondimensional beam deflection and critical velocity for simply-supported and fixed-fixed comparison.

Figure 2–14 is used to show where the maximum nondimensional deflection occurs along the moving loads main axis, the x–axis. The three-dimensional plot shows the maximum nondimensional displacement obtained throughout the beam's length for velocities below, at, and above the critical velocity. We see that the maximum nondimensional deflection for simply-supported boundary conditions occurs at the critical velocity at about 85% of the beam's total length ($0.85\,L$). Figure 2–15 is used to show where the maximum nondimensional deflection for fixed-fixed conditions. Here, we see that the maximum nondimensional deflection, occurs at about 77%.

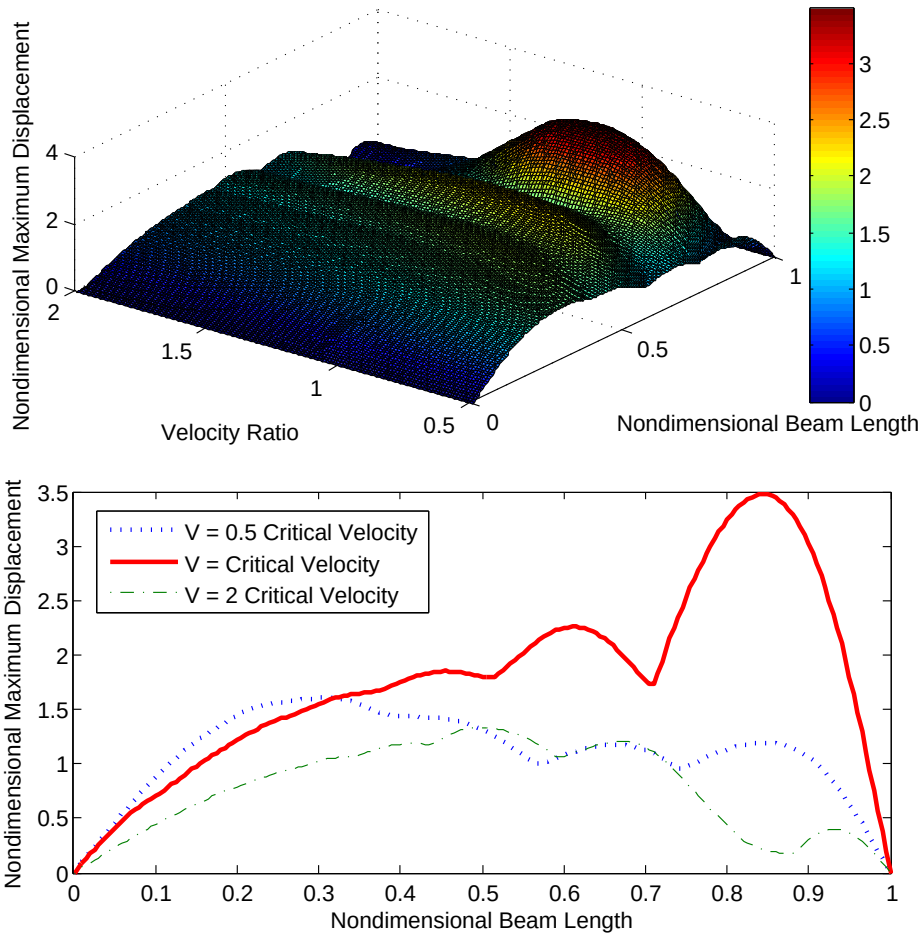

Figure 2–14: Maximum nondimensional beam deflection for simply-supported boundary conditions.

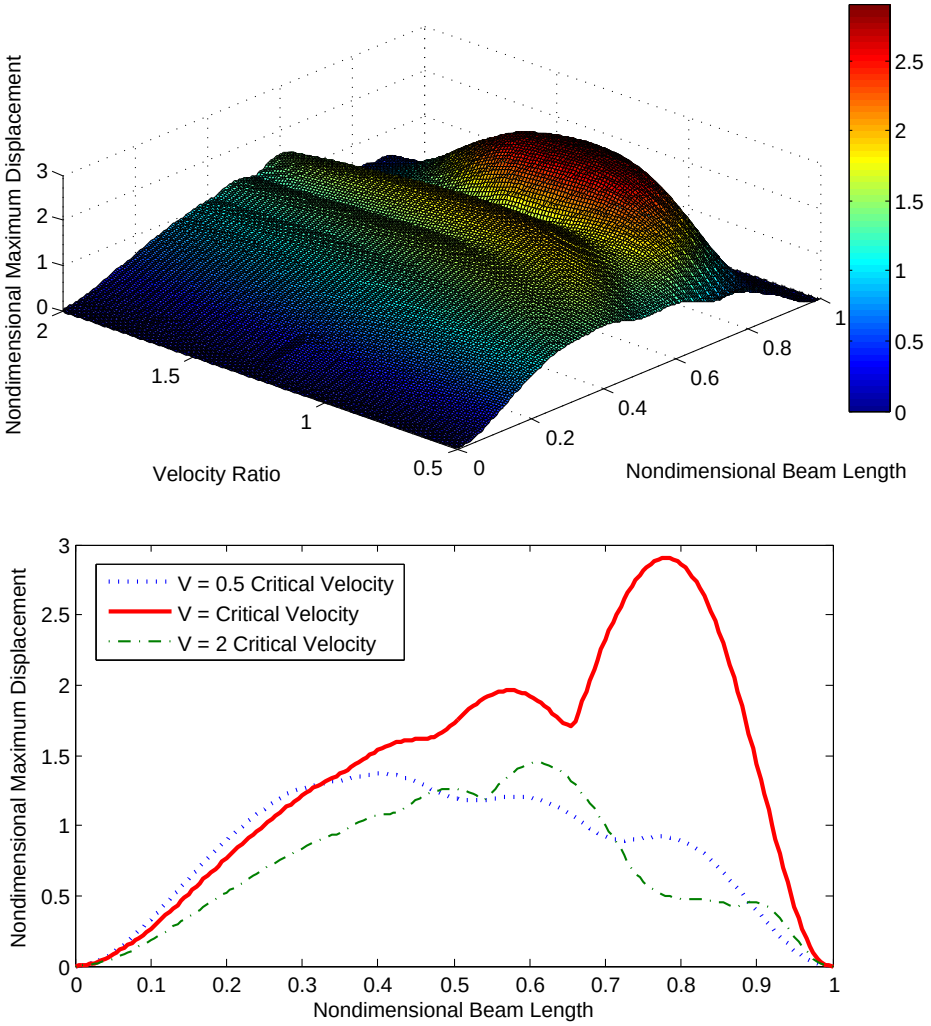

Figure 2–15: Maximum nondimensional beam deflection for fixed-fixed boundary conditions.

2.3.8 Effect of Different Load on the Critical Velocity

Figure 2–16 shows that the weight of the truck only influences the magnitude of the beam's deflection but not the value of the critical velocity. Recall that at the critical velocity the structure losses its stability and the deflection goes to infinity. It is assumed that the trucks were probably moving at about 75% of the critical velocity which would explain why the lake-ice did not break on their way to deliver the supplies. However, on their way back they were traveling at speeds exceeding the critical velocity which would have caused resonance and the unexpected lake-ice failure.

This is our explanation to the unsolved mystery of the *"Road of Life"* at Lake Ladoga. The possible explanation of why the slowly moving heavy trucks, fully loaded with supplies, did not crack the lake-ice and the unloaded trucks traveling faster did.

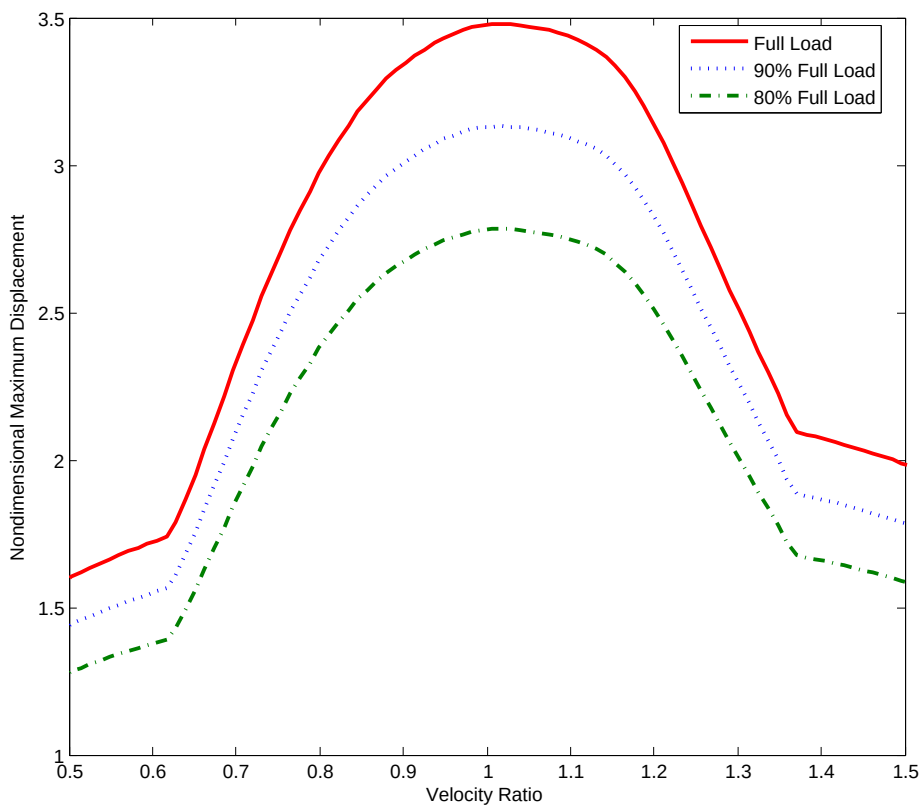

Figure 2–16: Beam's maximum nondimensional lake-ice deflection with different loads.

CHAPTER 3.
FEA OF UNEXPECTED FAILURE OF LAKE-ICE MODELED AS A VISCOELASTICALLY SUPPORTED PLATE SUBJECTED TO MOVING LOADS AT CRITICAL VELOCITY

In the previous chapter, we presented the finite element model to predict the unexpected failure of lake-ice when modeled as a viscoelastically supported beam subject to moving loads, here to do so for the plate with the same scenario. We develop the weak form of the equations of motion for plates and in an attempt to predict the unexpected failure of ice-water-truck structure at the critical velocity. The novelty of the approach consists of determining the ice-structure resonance at the critical velocity. We obtain the exact behavior when comparing the results against the analytical solution of steel plates when viscoelastically supported foundation under moving point loads. The plate and beam models, from the previous work, produced the same results. With this approach, we claim the first possible explanation for the *"Road of life"* at Lake Ladoga phenomena.

3.1 Background

From the literature, following two plate models are of our interest: (i) plates with elastic foundation, (ii) and plates with viscoelastic foundation. However, very little work is found in lake-ice behavior under moving loads when modeled as plate under elastic and viscoelastic foundations.

3.1.1 Elastically Supported Plate

The lake-ice beam, from our previous work, and plate models under moving loads is very useful for the Department of Transportation. The analysis of plates is not a new field and many researchers haver worked in the field [24, 29–39], especially using Fourier Transform. The so-called technique of "moving force" provides good

approximations for the vehicle-plate interaction when the vehicle-plate mass ratio is small (~ 0.15) or the vehicle travels at low speeds (13–209 m/s) [27]. It has been shown that the mode shape of plate deflection induced by a moving vehicle is different from the mode shape produced due to static forces. The partial differential equation of motion describing the dynamic response of an elastically supported plate under a moving load along the x-axis only is described by [24]:

$$\begin{aligned} D\left[\frac{\partial^4 w(x,y,t)}{\partial x^4} + 2\frac{\partial^4 w(x,y,t)}{\partial x^2 \partial y^2} + \frac{\partial^4 w(x,y,t)}{\partial y^4}\right] + \cdots \\ \cdots + \rho\, h\, \frac{\partial^2 w(x,y,t)}{\partial t^2} + c\, \frac{\partial w(x,y,t)}{\partial t} + k\, w(x,y,t) = P\, \delta(x - vt)\, \delta(y) \end{aligned} \tag{3.1}$$

Note that in the above equation, the units of k are [F/L^2] and c are [F/(L^2·s^2)]. Hence,

$$k = \rho_w\, g, \qquad c = \frac{0.5}{b}$$

Although plate models are more complete over the beam models as they provide us with a better understanding of the structure's behavior, in a few cases both models may capture the same behavior. As for an example, for velocities less than those of the critical, the deflected shapes are similar to those of the static case where the maximum displacement is obtained at the location of the load [31, 33]. For the mode shapes, in the moving direction, the maximum displacement increases with more pronounced fluctuations and the deflected region is more widely spread as the velocity increases [31, 33]. For the deflected shapes along the y-axis, the maximum displacement increases and the deflected region is also more widely spread as the velocity increases, but there are no additional fluctuations with increasing velocities.

The value of the foundational stiffness will influence the critical velocity. In fact, it is been shown that the critical speeds of a system increase with an increase in the values of the foundation modulus, whether or not the inertia of the load is considered. Moreover, these critical speeds are greater than those of rectangular plates not resting on an elastic foundation [29]. When the plate structure rests on a weak elastic foundation, almost the entire structure is affected by load and the resonant velocity is small. The area of the plate structure affected by the load

becomes narrower and resonant velocity becomes larger when the foundation stiffness increases [33].

There is some work done using the finite element analysis to study plates subjected to moving loads. Taheri et al. [28] compared the results obtained using finite elements against the results obtained using the structural impedance method [27]. They found that the rate of convergence for both methods is almost the same. FEM method has been also very useful for plates with various prescribed boundary conditions [28], demonstrating that the deflections of the simply-supported rectangular plate are higher than those of the simple-clamped plate.

Our major contribution is to present a FEM method regarding prediction of unexpected failure of lake-ice structures when elastically supported and subject to moving loads using the critical velocity to predict the loss of plate's stability.

3.1.2 Viscoelastically Supported Plate

The dynamic behavior of a viscoelastically supported plate under moving loads has been previously studied [28, 31, 33]. The damping the decrease the maximum amplitude in the x-direction (the direction of the moving load) and creates a *lag* between the position of the maximum displacement and the location of the load. This behavior has not been observed in the y-direction, where the damping has very little effect on the maximum displacement.

3.1.3 Moving Loads on lake-ice

Frozen lakes and oceans had been used as a transportation medium for decades, and are still being used, especially in the Arctic. There has been a number of experimental researches conducted in an attempt to determine the behavior of ice sheets under moving loads. The results of these experimental showed that the behaviors captured by the theoretical beam and plate models are similar when compared to the data.

In 1955, over the Mille Lacs field, a deflectometer was used to measure the lake-ice displacement caused by a moving vehicle across the field. It was noticed that at slower speeds the behavior resemble a simple static deflection profile and that this deflection increased with the vehicle's velocity until the sheet reaches its

maximum deflection of 2.5 times the static value. This maximum deflection occurs when the vehicle reaches the critical velocity [41], which varies significantly with the ice conditions [44]; after this, the deflection begins to decrease. At this speed, the deflection profile becomes wavelike, with short waves ahead of the load and longer waves behind it [41]. Similar results were obtaining in other scenarios showing a low amplification factor of 2.8, suggesting that inelastic processes were present [43].

Squire et al. [9] did a lot of work of moving loads over ice structures using testing facilities. Most of their work is focused on moving loads over floating ice sheets. They presented some analytical models, validated by test data. However, very little work has been done in predicting failure of lake-ice plates resting on water using analytical or finite element models at the resonant speed. This is the main motivation of our work that to provide a computational model to predict unexpected lake-ice failure.

3.2 Computational model

As we previously mentioned, the main goal of this work is try to solve the phenomena around the *"Road of life"* at Lake Ladoga. Here, we will use the critical velocity as the basis to try to solve this problem. We will do so by modeling the ice-structure as elastic and viscoelastically supported plate.

3.2.1 Elastically Supported Plate: Analytical

Before we proceed to develop our finite element model, let us derive an analytical expression for the critical velocity of an elastically supported plate under the effect of a moving load in the x-direction. Let us start with the plate equation of motion without damping, from Eq. 3.1, which is:

$$\begin{aligned} D\left[\frac{\partial^4 w(x,y,t)}{\partial x^4} + 2\frac{\partial^4 w(x,y,t)}{\partial x^2 \partial y^2} + \frac{\partial^4 w(x,y,t)}{\partial y^4}\right] + \cdots \\ \cdots + \rho\, h\, \frac{\partial^2 w(x,y,t)}{\partial t^2} + k\, w(x,y,t) = P\, \delta(x - vt)\, \delta(y) \end{aligned} \tag{3.2}$$

Let us assume a solution to the transverse deflections as following:

$$w(x,y,t) = c_1\, e^{i(N_1(x-vt)+N_2(y-vt))} \tag{3.3}$$

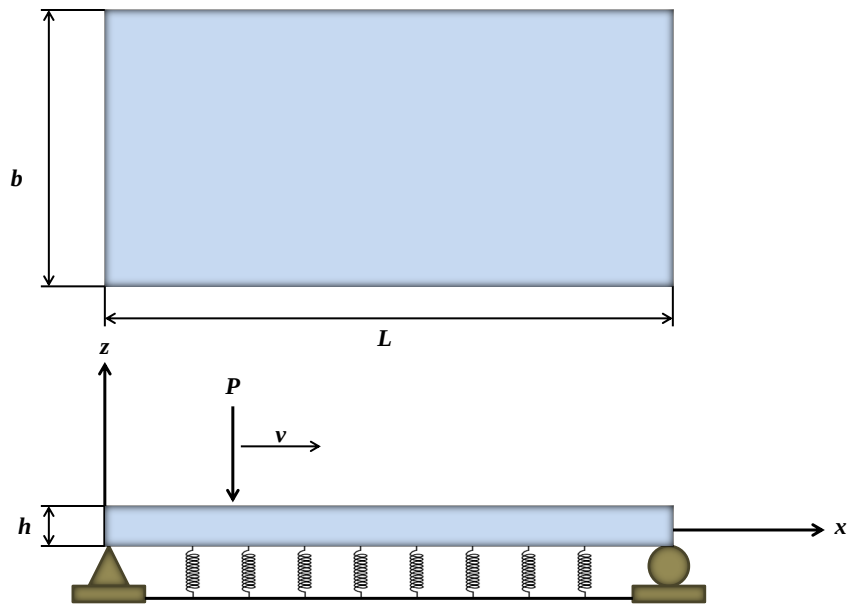

Figure 3–1: Simply supported plate over elastic foundation with moving load.

Since we assumed no motion in the y direction, Eq. 3.3 reduces to

$$w(x,t) = c_1\, e^{i(N_1(x-vt))} \tag{3.4}$$

where c_1 is a constant representing deflection amplitude and N_1 is a real number. Substituting Eq. 3.4 into Eq. 3.2 and simplifying we get the following expression:

$$D\, N_1^4 + \rho\, h\, V^2\, N_1^2 + k\, w = 0 \tag{3.5}$$

Denoting $N_1^2 \equiv Z$, Eq. 3.5 can be presented as a quadratic equation

$$D\, Z^2 + \rho\, h\, V^2\, Z + k\, w = 0 \tag{3.6}$$

whose roots are:

$$N_1^2 = Z_{1,2} = \frac{\rho\, h\, V^2 \pm \sqrt{\rho^2\, h^2\, V^4 - 4\, D\, k}}{2\, D} \tag{3.7}$$

Recall, that N_1 was assumed to be real number, hence, Eq. 3.7 requires that the squared expression be positive or equal to zero, i.e.,

$$\sqrt{\rho^2 h^2 V^4 - 4Dk} \geq 0 \quad \rightarrow \quad v_{cr} = \sqrt{\frac{2\sqrt{Dk}}{\rho h}} = \sqrt[4]{\frac{E\, g\, h}{3\, \rho\, (1-\nu^2)}} \tag{3.8}$$

The above derivation is identical as the one recommended by Hsi-Ming [39] who recommended to use the same beam expression but replacing EI by D [39]. Equations 2.14 and 3.8 show that the critical velocity for plates is slightly higher than the one calculated for beam. This is mainly because of the inclusion of the Poisson's ratio.

3.2.2 Elastically Supported Plate: FEA

In order to develop the finite element model, we develop the weak form of Eq. 3.2 and then discretize the model using quadrilateral elements, shown in Fig. 3–2.

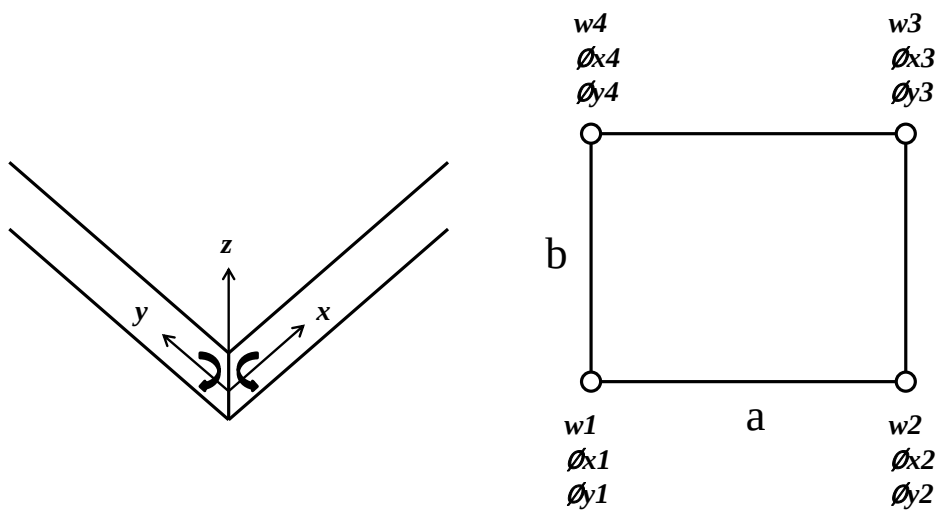

Figure 3–2: Rectangular finite element.

We find the weak form of Eq. 3.2 by multiplying it by a weighted function ϑ, integrating it over the domain and finally using the Green's Theorem to get:

$$\begin{aligned}\iint_{\Omega^e} \Bigg\{ \frac{\partial^2 \vartheta}{\partial x^2}\left(D\frac{\partial^2 w}{\partial x^2} + \frac{\partial^2 w}{\partial y^2}\right) + \frac{\partial^2 \vartheta}{\partial y^2}\left(D\frac{\partial^2 w}{\partial x^2} + \frac{\partial^2 w}{\partial y^2}\right) + \cdots \\ \cdots + \vartheta\,\rho\,h\frac{\partial^2 w}{\partial t^2} + \vartheta\,k\,w - P\,\delta(x - vt)\,\delta(y)\Bigg\}\,dx\,dy = 0\end{aligned} \tag{3.9}$$

We assume that the approximate displacement function is:

$$w = \sum_{j=1}^{n} \Delta_j^e(t_s)\phi_j^e(\bar{x},\bar{y}) = \sum_{j=1}^{n} (\Delta_j^s)^e \phi_j^e(\bar{x},\bar{y}) \tag{3.10}$$

where $(\Delta_j^s)^e$ is the value of $w(\bar{x}, \bar{y}, t)$ at time $t = t_s$ and at node j of the element e. By substituting $\vartheta = \phi_i(\bar{x}, \bar{y})$ and Eq. 3.10 into Eq. 3.9 we get:

$$\begin{aligned}\iint_{\Omega^e} \Bigg\{ D \Bigg[\frac{d^2\phi_i}{d\bar{x}^2} \left(\sum_{j=1}^{n} \Delta_j^e \frac{d^2\phi_j}{d\bar{x}^2} + \frac{d^2\phi_j}{d\bar{y}^2} \right) + \cdots \\ \cdots + \frac{d^2\phi_i}{d\bar{y}^2} \left(\sum_{j=1}^{n} \Delta_j^e \frac{d^2\phi_j}{d\bar{x}^2} + \frac{d^2\phi_j}{d\bar{y}^2} \right) \Bigg] + \cdots \\ \cdots + \phi_i \, \rho \, h \left(\sum_{j=1}^{n} \frac{d^2 \Delta_j^e}{dt^2} \phi_j \right) + \phi_i \, k \, \Delta_j^e \, \phi_j - P \, \phi_i \Bigg\} \, d\bar{x} \, d\bar{y} = 0\end{aligned} \tag{3.11}$$

Conveniently, we express it in its matrix form as follows:

$$[K] \, \Delta^e + [M] \, \ddot{\Delta}^e = \{F\} \tag{3.12}$$

where

$$\begin{aligned}[K] &= \int_0^a \int_0^b \left\{ D \left[\frac{d^2\phi_i}{d\bar{x}^2} \left(\frac{d^2\phi_j}{d\bar{x}^2} + \frac{d^2\phi_j}{d\bar{y}^2} \right) + \frac{d^2\phi_i}{d\bar{y}^2} \left(\frac{d^2\phi_j}{d\bar{x}^2} + \frac{d^2\phi_j}{d\bar{y}^2} \right) \right] + k\phi_i\phi_j \right\} d\bar{y} \, d\bar{x} \\ [M] &= \int_0^a \int_0^b \rho \, h \, \phi_i \, \phi_j d\bar{y} \, d\bar{x} \\ \{F\} &= \int_0^a \int_0^b P \, \phi_i d\bar{y} \, d\bar{x}\end{aligned}$$

3.2.3 Viscoelastically Supported Plate: FEA

For the case of viscoelastically supported plate, we use Eq. 3.1 that includes the damping. Using a similar approach as for the elastically supported plate, the weak form is

$$\begin{aligned}\iint_{\Omega^e} \Bigg\{ \frac{\partial^2\vartheta}{\partial\bar{x}^2} \left(D \frac{\partial^2 w}{\partial\bar{x}^2} + \frac{\partial^2 w}{\partial\bar{y}^2} \right) + \frac{\partial^2\vartheta}{\partial\bar{y}^2} \left(D \frac{\partial^2 w}{\partial\bar{x}^2} + \frac{\partial^2 w}{\partial\bar{y}^2} \right) + \cdots \\ \cdots + \vartheta \, \rho \, h \, \frac{\partial^2 w}{\partial t^2} + \vartheta \, c \, \frac{\partial w}{\partial t} + \vartheta \, k \, w - P \, \vartheta \Bigg\} \, d\bar{x} \, d\bar{y} = 0\end{aligned} \tag{3.13}$$

After substituting the approximate displacement function, Eq. 3.10, into Eq. 3.13 we can express the weak form in its matrix form as follows:

$$[K] \, \{\Delta^e\} + [M] \, \{\ddot{\Delta}^e\} + [C] \, \{\dot{\Delta}\} = \{F\} \tag{3.14}$$

where the only new component is the damping term and is defined as follows:

$$[C] = \int_0^a \int_0^b c\,\phi_i \phi_j \, d\bar{y}\, d\bar{x} \tag{3.15}$$

We do not discuss the Newmark's time integration scheme because it was described in Section 2.2.5 for the case of beam models and it applies to plate models as well.

3.2.4 2D Moving Finite Element Method

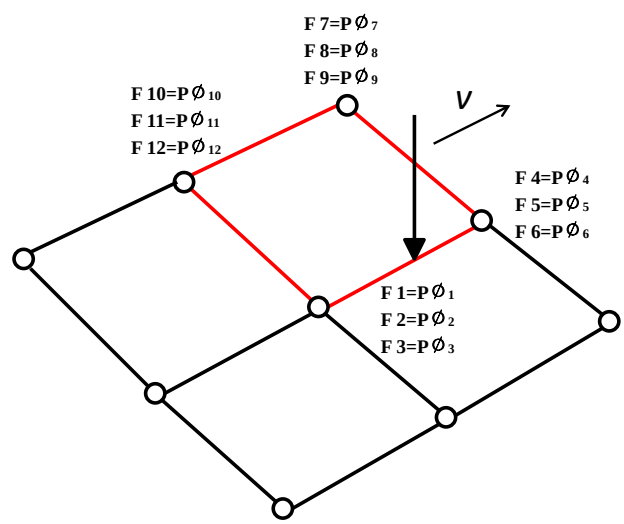

Figure 3–3: Moving Finite Element of the 2D element e.

Here we plan to explain our approach to the 2D moving finite element (MFE) method which has been previously developed [47, 48] and modified by us. We start by stating that the forces on all the nodes of the plate are zero with the exception of the nodes of element e that are subjected to the concentrated moving load P. Thus, the force vector will take the following form:

$$\begin{aligned}\{F\} = \{0\,0 \cdots F_1^e(t)\, F_2^e(t)\, F_3^e(t)\, F_4^e(t)\, F_5^e(t)\, F_6^e(t)\, F_7^e(t)\, F_8^e(t) \cdots \\ \cdots F_9^e(t)\, F_{10}^e(t)\, F_{11}^e(t)\, F_{12}^e(t) \cdots 0\,0\,0\}\end{aligned} \tag{3.16}$$

where F_i^e (for $i = 1, \ldots, 12$) represents the equivalent nodal forces of the element e where the force is applied,

$$\begin{aligned}\{F^e(t)\} = \{F_1^e(t)\, F_2^e(t)\, F_3^e(t)\, F_4^e(t)\, F_5^e(t)\, F_6^e(t)\, F_7^e(t)\, F_8^e(t) \cdots \\ \cdots F_9^e(t)\, F_{10}^e(t)\, F_{11}^e(t)\, F_{12}^e(t)\}^{\mathrm{T}} = P\{\phi\}\end{aligned} \tag{3.17}$$

and $\phi_i(\bar{x}, \bar{y})$ (for $i = 1, \ldots, 12$) represents the elemental shape functions. Figure 3–3 shows that the elements and nodes of the plate that are subjected to the concentrated force that cannot be zero. It can be further seen that for our case, we placed the force in the lower edge of the element. Therefore, the x position of the concentrated load P in the element is varying while the y position remains constant.

Similar to the beam model, this x position of the load is defined as

$$x_p = V\, r\, \Delta t \tag{3.18}$$

and the element e where the moving concentrated force is applied at any time t can be know from

$$e = \left(\text{The integer part of } \frac{x_p(t)}{a} \right) + 1 \tag{3.19}$$

Again, the shape functions $\phi_i(\bar{x}, \bar{y})$ are written in term of this local coordinated. Thus the shape functions are redefined as $\phi_i(\varsigma)$, making the shape functions depending of ς instead of x and y, where ς is defined as

$$\varsigma = \frac{x_p(t) - (e-1)a}{a} \tag{3.20}$$

where a is the length of the plate element in the x-coordinate. It should be noted that based on the fact that y remain constant for the hole time Δt, ς depends only of x.

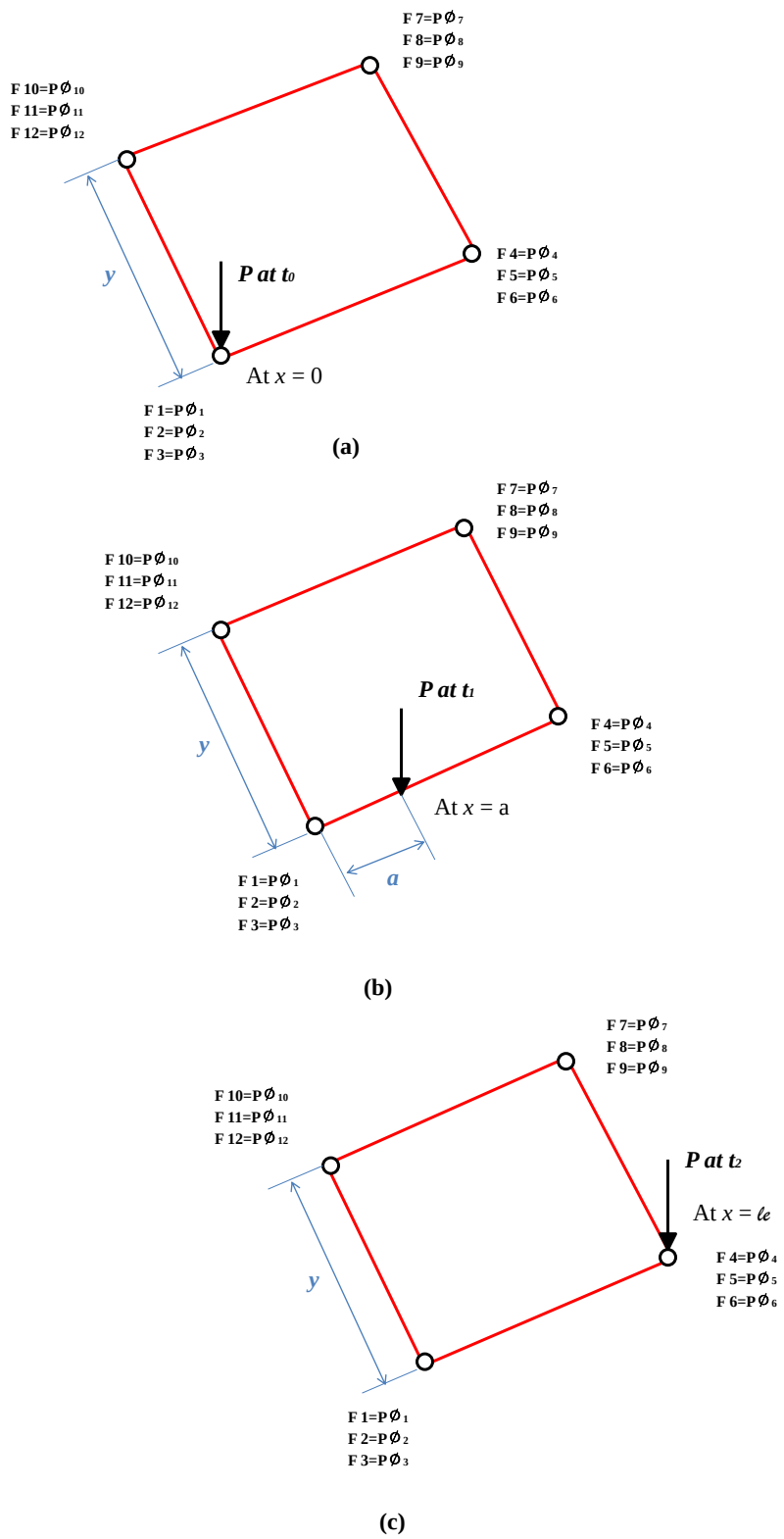

Figure 3–4: The equivalent forces of the 2D element e subjected to a moving load P.

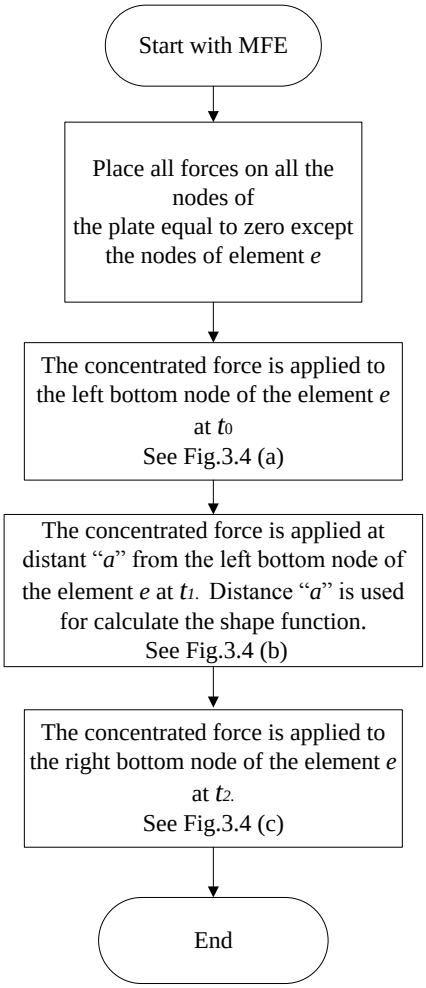

Figure 3–5: Moving Finite Element approach for a 2D element e.

3.3 Results and Discussions

3.3.1 Convergence Plot

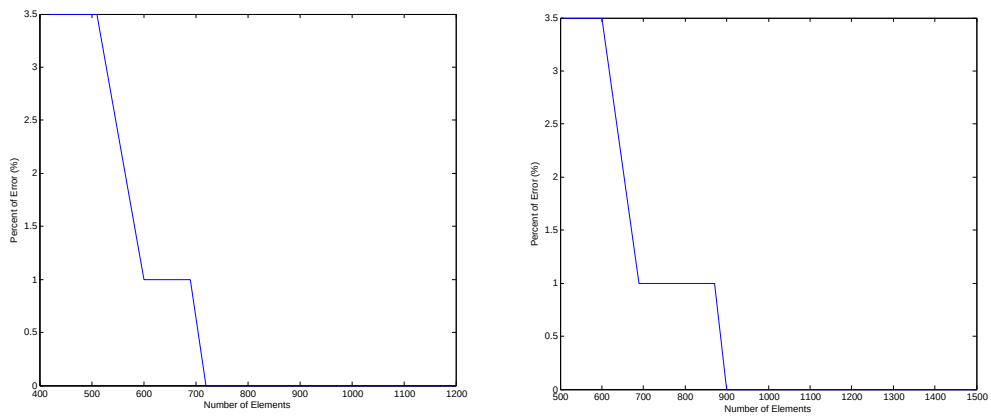

Figure 3–6: Finite element convergence plot for the critical velocity for the plate elastic (left) and viscoelastically (right) supported.

Figure 3–6 shows that we need 720 elements to reach convergence for the elastically supported lake-ice and 900 elements for the viscoelastically supported lake-ice. Hence, there is no need to use a finer mesh than that of 900 elements. However, we ran all our analysis using 1200 elements to ensure convergence throughout our analysis.

3.3.2 Effect of the Elastic Foundation on the Critical Velocity

First, we wanted to study the influence of the elastic foundation on the critical velocity. When we validated our model with the behavior of the hypervelocity rail presented by Nechitailo and Lewis [3], we found that the mayor difference was the transition from the quasi-static regime to the resonant regime. For the truck-ice-water structure, that regime occurs gradually. Figure 3–7 shows a very similar behavior compared with the beam model. Results show that a higher elastic foundation will produce a smaller nondimensional maximum deflection and a slightly higher critical velocity. This behavior matches the one obtained in the beam model.

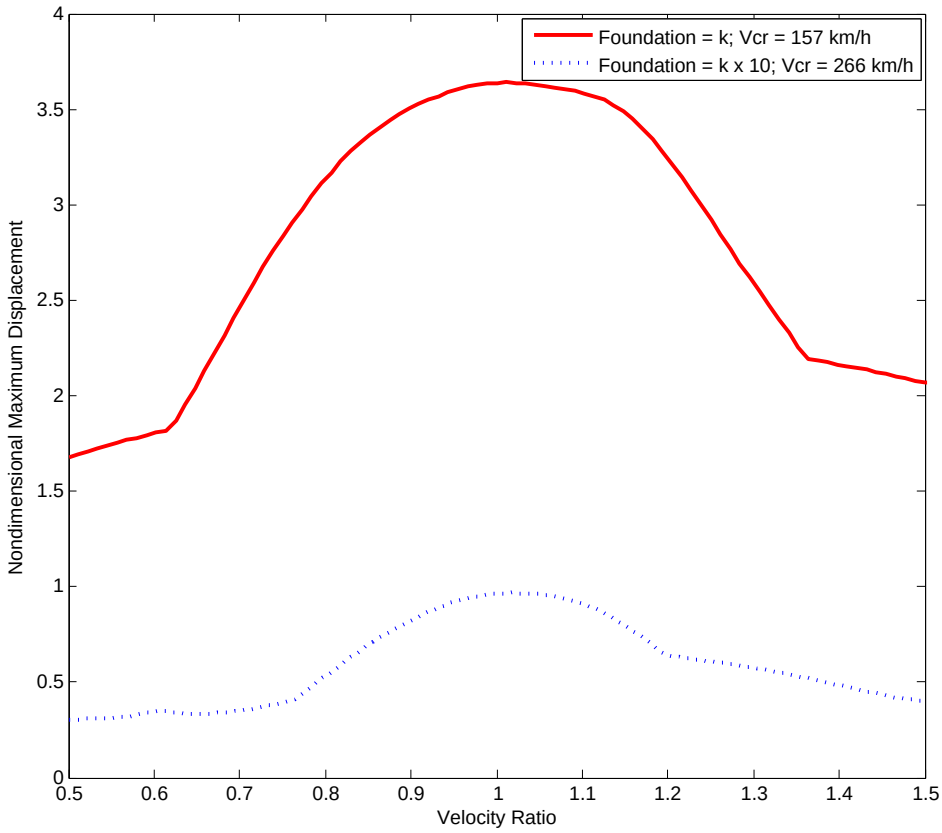

Figure 3–7: Plate's maximum lake-ice deflection with different elastic foundations.

3.3.3 Effect of damping on the Critical Velocity

Next, we studied the effect of the viscoelastic foundation on the critical velocity. Figure 3–8 shows, as it was the case of the beam model, that the damping coefficient of the water is too small to make significant changes on the critical velocity. These results are in agreement with those found through experimental data by Kim et al. [31], Taheri et al [28] and Huang et al,[33] who concluded that the damping coefficient will have an effect on the maximum deflection but not on the critical velocity. Also, as presented in the previous chapter, a water damping factor of $0.5/b$ is too small to mitigate large amplitudes and resonance effects of the moving load over ice.

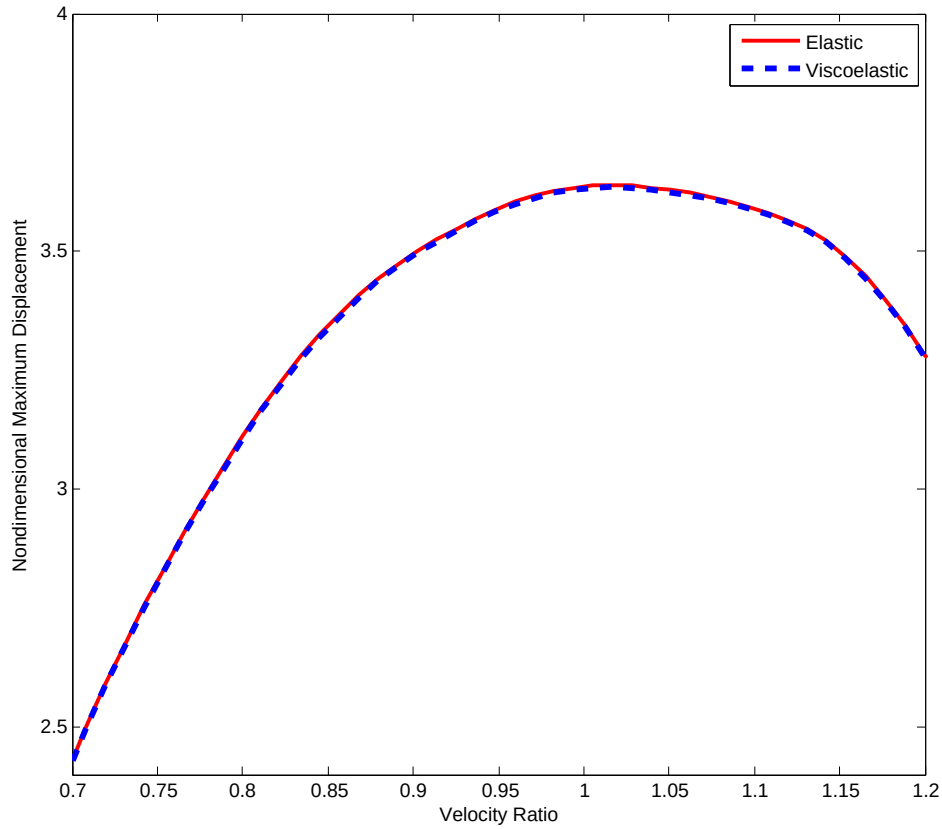

Figure 3–8: Maximum nodimensional plate deflection of lake-ice when water is modeled using an elastic and viscoelastic foundation.

3.3.4 Maximum Plate Deflection Analysis at the Critical Velocity

In this section, we study how the critical velocity affects the plate's mode shape. Figure 3–9 shows the mode shape obtained when the load travels at half of the critical velocity in the direction of the moving load ($y = 0$). These results show that for velocities less than the critical one, the deflected plate shows a similar behavior to that of the static case where the maximum displacement is obtained where the load is located, which is expected since no resonance has occurred. Also, when we compare the mode shape of the plate model to the one in the beam model, we see that the plate model has more similarity compared to the static case. It almost seems like the beam model would be incorrect. In fact it is not, it is giving the results for $y = 0.5$ for the plate model. As we decrease the ration b/L we would see that both results coalesce. In this context, we see that the plate model has better prediction when compared with the beam model, which is expected for such a high b/L ratio.

When the load's velocity approaches the critical value, the frequency of fluctuations in front of the load increases compared with the fluctuations behind the load, showing a "resonance-effect", as shown in Fig. 3–10. The behavior is similar to that of the beam model. The difference of the mode shapes in both models is because, as discussed earlier, the plate captures the behavior better that the beam model.

Figure 3–11 shows that the plate's mode shape at twice the critical velocity. We see that as the velocity continues increasing above the critical velocity, the frequency of the fluctuations in front of the load increases as well, and the amplitudes of the fluctuations in front of the load are smaller than those behind the load. This shows that indeed there is a resonance-effect at the critical velocity.

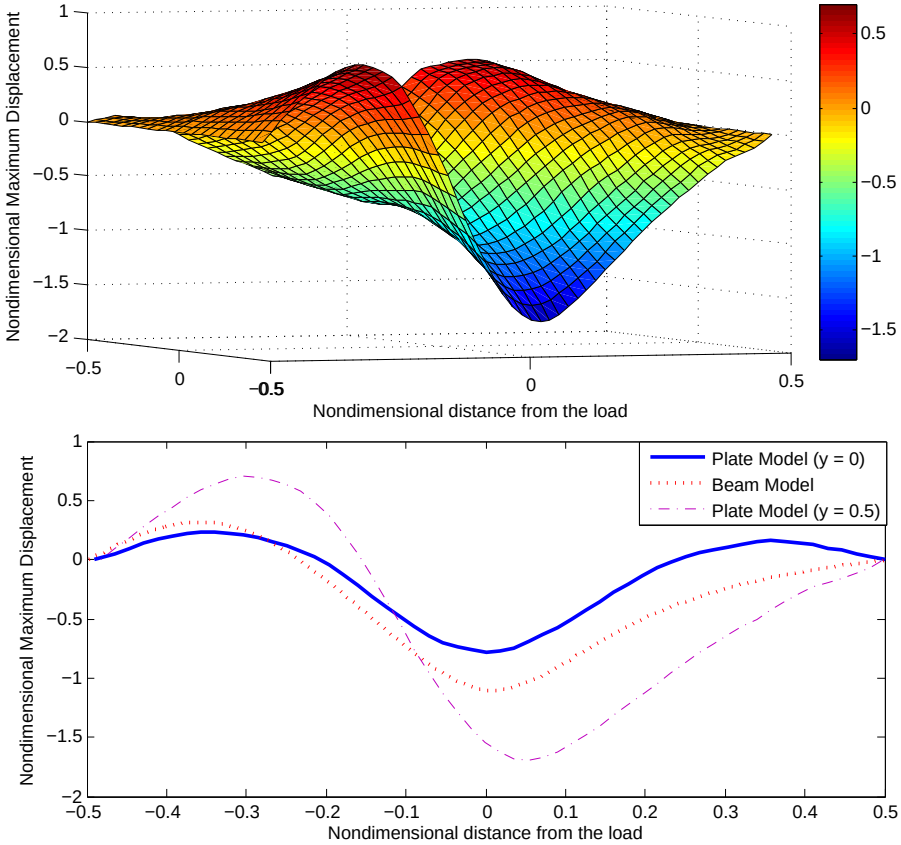

Figure 3–9: Mode shapes from the beam and plate models at half critical velocity.

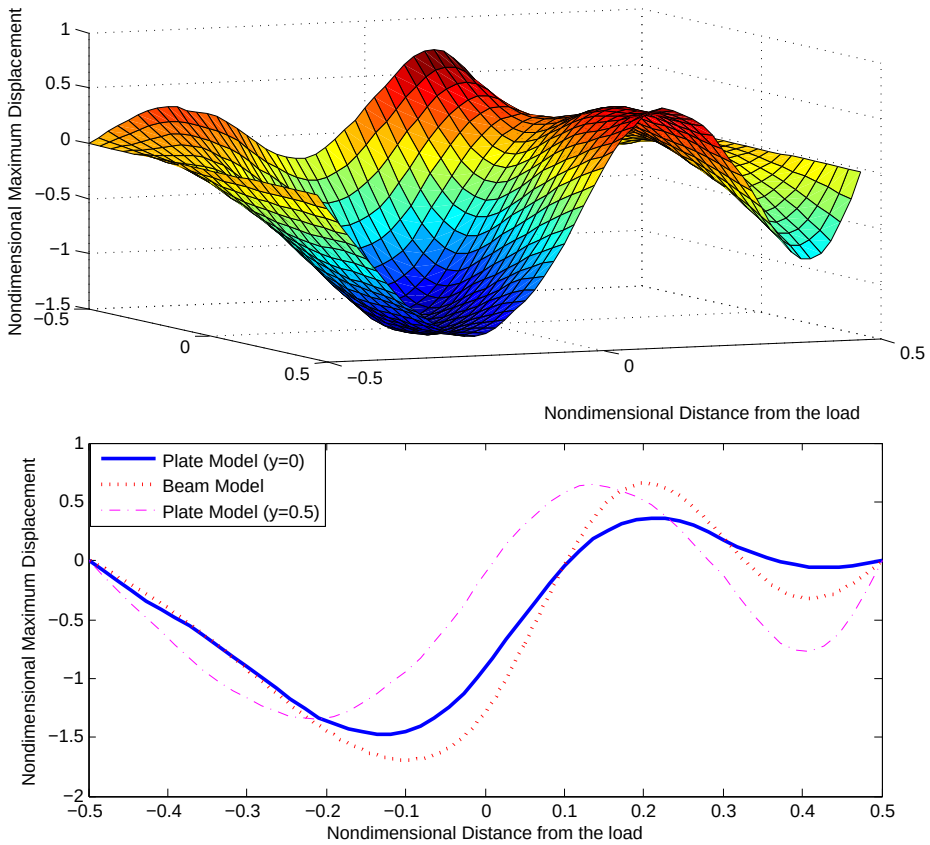

Figure 3–10: Mode shapes from the beam and plate models at critical velocity.

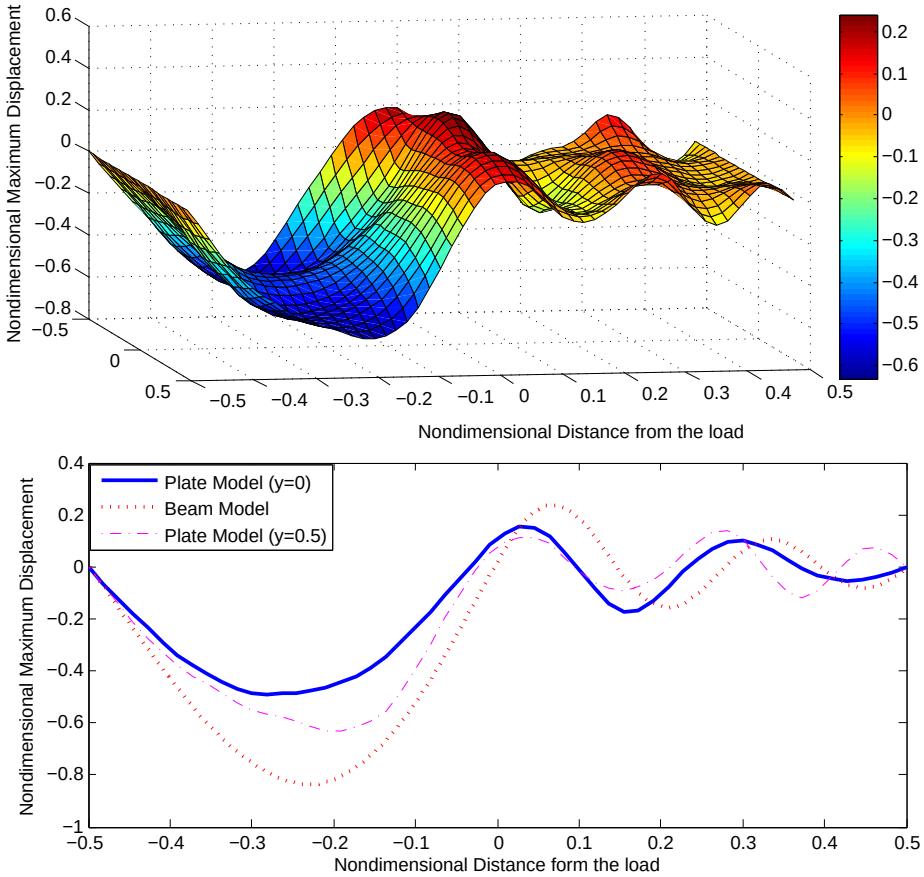

Figure 3–11: Mode shapes from the beam and plate models at twice critical velocity.

3.3.5 Effect of Different Boundary Conditions on the Critical Velocity

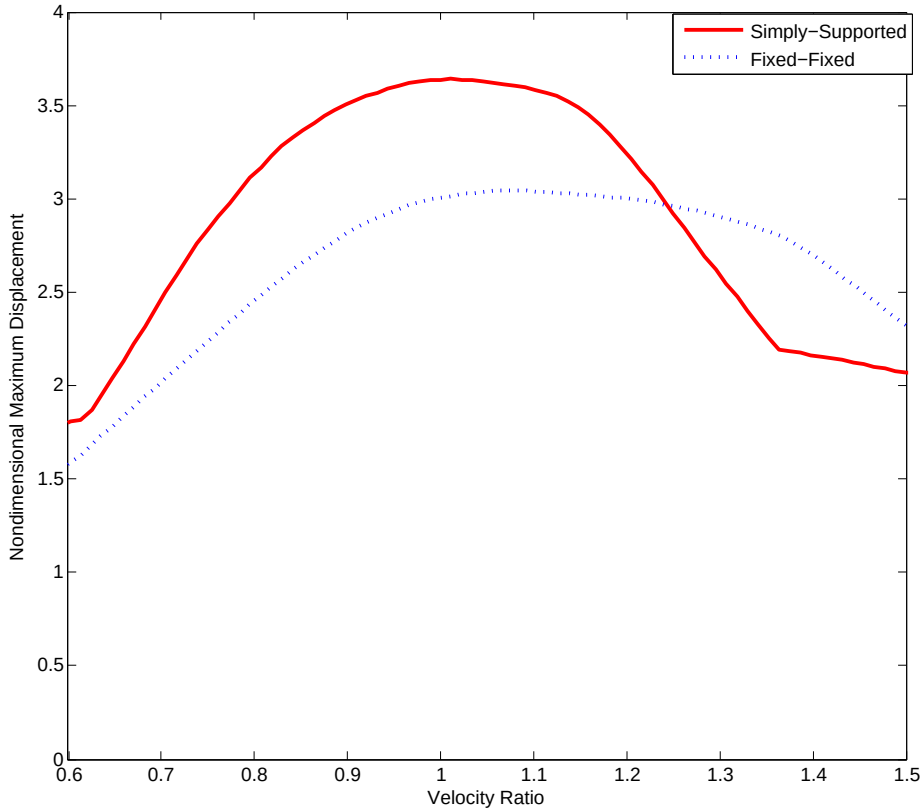

Figure 3–12: Maximum nondimensional plate deflection and critical velocity for simply-supported and fixed-fixed comparison.

As it was in the case of the beam, we first modeled our lake-ice structure using a simply-supported boundary conditions at $x = -L/2, L/2$ and free-end boundary conditions at $y = -b/2, b/2$. However, as discussed in Chapter 1, the most-realistic boundary conditions for our problem should be fixed-fixed boundary conditions at $x = -L/2, L/2$. Figure 3–12 shows the comparison between the simply-supported and fixed-fixed boundary conditions at $x = -L/2, L/2$. We see that the maximum nondimensional deflection for the simply-supported boundary ($y = 0$) occurs at about 157 km/h and for fixed-fixed boundary ($y = 0$) occurs at 163 km/h which is a 3% difference. Hence, when modeling the lake-ice as a plate, either boundary condition will produce the resonance effect for roughly the same critical velocity.

3.3.6 Effect of Different Load on the Critical Velocity

Figure 3–13 shows similar results when compared with those obtained by the beam model. It reinforces the conclusion that the critical velocity does not depend on the load size. Hence, we reiterate that the trucks were probably moving at about 75% of the critical velocity on their way to deliver the supplies and did not break the lake-ice. However, on their way back they were traveling at speeds higher that the critical one which would have caused resonance and the unexpected lake-ice failure. This is our explanation to the unsolved mystery of the *"Road of Life"* at Lake Ladoga. Figure 3–14 shows that both plate and beam models for this problem produce the same critical velocity.

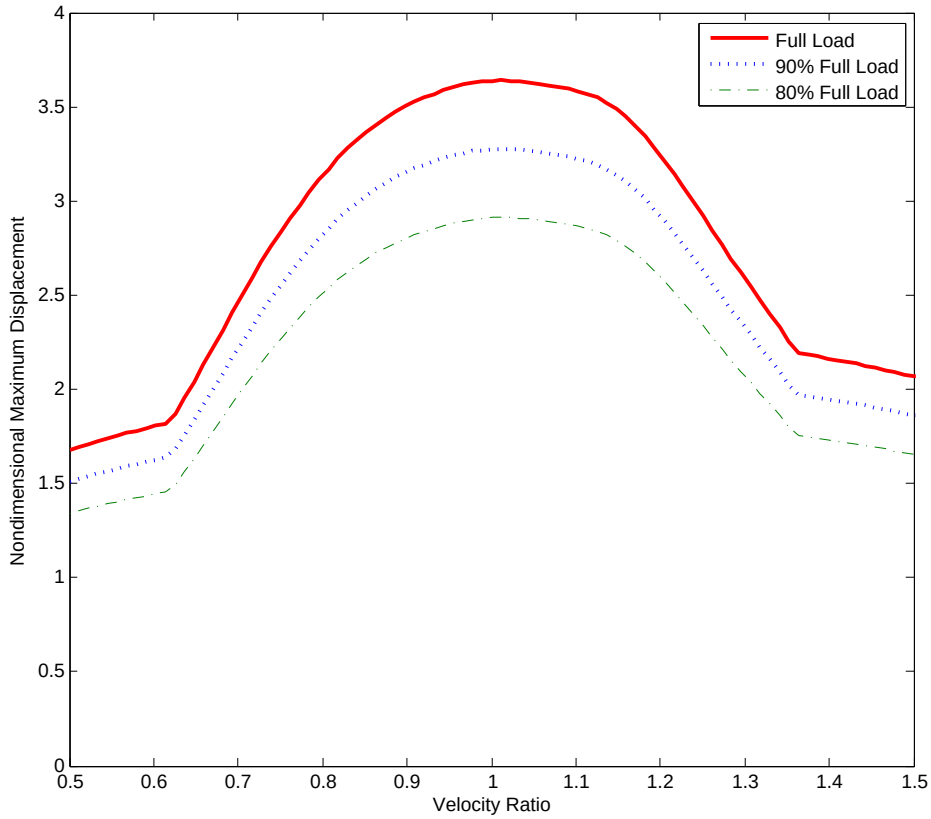

Figure 3–13: Plate's maximum nondimensional lake-ice deflection with different loads.

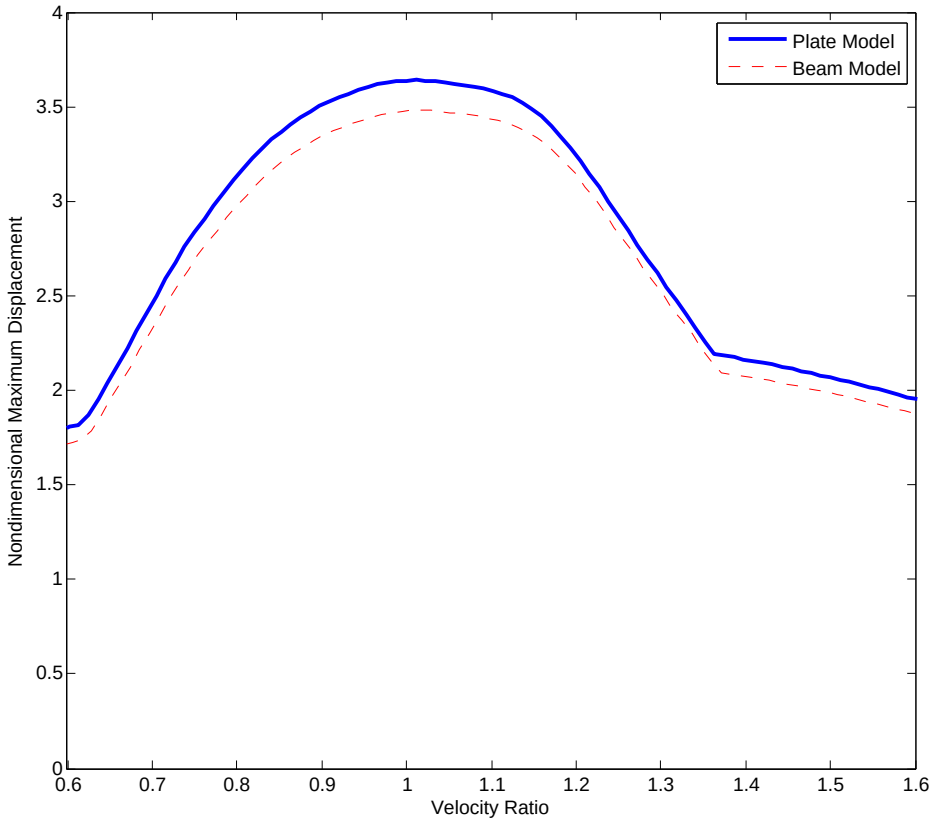

Figure 3–14: Maximum nondimensional lake-ice deflections for the beam and plate models.

CHAPTER 4.
FINAL REMARKS

4.1 Conclusion

In this work, we used a finite element-based dynamic response approach to determine the nature of the unexpected failure of lake-ice at the critical velocity. The results of our model against the analytical solutions provided the exact solution whereas no other finite element software was able to do so. Results show that when the moving load reaches values around the critical velocity, a resonant regime is present and is independent of the load size. Also, the transition from the quasi-static regime to a resonant regime occurs gradually, showing that the resonant regime's presence depends also on the stiffness and damping properties of the water. The results for the viscoelastic case show that the water viscosity does not play a big role in the critical velocity. Through this work, we developed a novel approach to predict the unexpected lake-ice failure at critical velocity using the finite element method and we propose the first promising explanation for the Lake Ladoga mystery. The solved mystery is that the slow and heavy trucks did not break the lake-ice, but once the cargo was delivered, the lighter trucks drove back at higher speeds reaching velocities near the critical, creating unexpected failure of the lake-ice.

4.2 Future Work and Recommendation

There is plenty of room to expand this work and of great interest to the Department of Transportation and military agencies as they continue to use lake-ice as transportation roads. First of all, we assumed that the moving load velocities were constant as they crossed the lake-ice; however the fact is that this may not be true. This would lead to a complex time-varying system in which it would be very interesting to see how the critical velocity would change.

Another, are of expansion would be to approximate the ice thickness using some probabilistic model allowing the engineers to learn how ice thickness would help or weaken the ice-water system. Further, we assumed throughout this work that the ice rested completely over ice, which is absolutely not accurate. It would be interesting to show how the partially submerged ice would affect the results by developing a three dimensional finite element model for this purpose.

Another subject for study is the case where the moving load is producing a harmonic moving load instead of the static one studied in this work. Previously, Seong-Min et al. [25] studied the effect of a moving harmonic load. They showed that for a moving harmonic load, the critical frequency decreases with an increase in velocity for velocities smaller than critical and the reverse occurs for velocities larger than this critical velocity. For load frequencies smaller than the critical frequency of a stationary harmonic load, there are two critical velocities defined as follow [25]:

$$v_{cr1} = v_{cr}\left(1 - \frac{\bar{f}}{f_{cr0}}\right)^{\frac{7}{10}} \tag{4.1}$$

$$v_{cr2} = v_{cr}\left(1 + \frac{\bar{f}}{f_{cr0}}\right)^{\frac{2}{3}} \tag{4.2}$$

$$f_{cr0} = \frac{1}{2\pi}\sqrt{\frac{k}{\rho A}} \tag{4.3}$$

where $\bar{f}$ is the frequency of the moving harmonic load in hertz and f_{cr0} the critical frequency of a stationary harmonic load ($v = 0$). Note that the critical frequency, f_{cr0} is independent of the flexural rigidity of the beam and the size of the loaded length. Equations 4.1 and 4.2 show that as the load frequency increases, the first critical velocity decreases and the second increases. For load frequencies larger than the critical frequency of a stationary harmonic load, only the second critical velocity exists. Now, we may solve equations 4.1 and 4.2 for the critical frequencies: For load velocity $(v) \leq v_{cr}$

$$f_{cr} = f_{cr0}\left[1 - \left(\frac{v}{v_{cr}}\right)^{1.43}\right] \tag{4.4}$$

For load velocity $(v) \geq v_{cr}$

$$f_{cr} = f_{cr0}\left[\left(\frac{v}{v_{cr}}\right)^{\frac{3}{2}} - 1\right] \tag{4.5}$$

One last suggest area of expansion is of including the blowing air on top of the ice creating an aeroelastic type of effect. This aeroelastic behavior will definitely influence the critical speed as resonance regimens will be shifted.

APPENDICES

APPENDIX A.
ANALYTICAL SOLUTION FOR THE ELASTICALLY SUPPORTED BEAM

In Chapter 2, we mentioned the solution to the following equation of motion for an elastically supported beam:

$$EI\,\frac{\partial^4 w(x,t)}{\partial x^4} + \rho\,A\,\frac{\partial^2 w(x,t)}{\partial t^2} + k\,w(x,t) = P\,\delta(x - vt) \tag{A.1}$$

Here we plan on showing the step-by-step solution to the above equation. Let us start by dividing in both sides of Eq. A.1 by EI and defining two new parameters (for ease of derivation) $n^2 = k/EI$ and $m = \rho/2EI$. By doing so, we get:

$$\frac{\partial^4 w(x,t)}{\partial x^4} + 2\,m\,A\,\frac{\partial^2 w(x,t)}{\partial t^2} + n^2\,w(x,t) = \frac{P}{EI}\,\delta(x - vt). \tag{A.2}$$

Now, the transverse deflections of a beam subjected to a moving load can be sought using the following expression

$$w(x,t) = \int_{-\infty}^{\infty} w^*(\gamma,t) e^{-i\gamma x} d\gamma. \tag{A.3}$$

where

$$w^* = \int_{-\infty}^{\infty} w(x,t)\,e^{-i\gamma x}\,dx \tag{A.4}$$

Equations A.4 and A.3 constitute a Fourier transformation pair. Let us multiply both sides of Eq. 2.6 by $e^{-i\gamma x}$ and integrate by parts over x from $-\infty$ to $+\infty$, and assuming that the space derivatives of w vanish at $x = \pm\infty$, we get:

$$\gamma^4\,w^* + n^2\,w^* + 2\,m\,\frac{d^2 w^*}{dt^2} = \frac{P}{EI}\,e^{-i\gamma vt}. \tag{A.5}$$

After substituting $w^* = W^* e^{-i\gamma vt}$ in Eq. A.5, we get the following expression:

$$\left(\gamma^4 + n^2 - 2\,m\,v\,\gamma^2 v^2\right)\,W^* = \frac{P}{EI} \tag{A.6}$$

Now, Eq. A.3 becomes:

$$w(x,t) = \frac{P}{EI}\frac{1}{2\pi}\int_{-\infty}^{\infty}\frac{e^{i\gamma(x-vt)}}{\gamma^4 - 2mv^2\gamma^2 + n^2}d\gamma \tag{A.7}$$

or

$$w(x,t) = \left(\frac{P}{EI}\right)\left(\frac{1}{2\pi}\right)2\pi i\sum \mathrm{R}, \tag{A.8}$$

where **R** are the residues at four simple poles γ_1 to γ_4, shown in Fig. A–1.

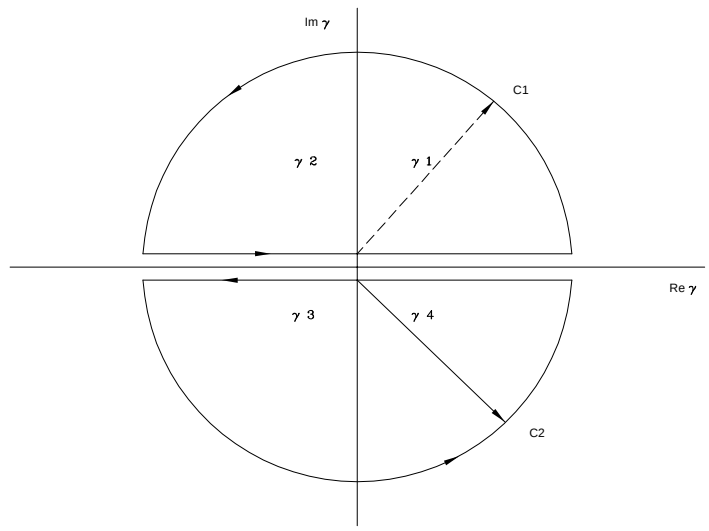

Figure A–1: Position of poles.

In order to find the residue calculation, let us use the following expression:

$$q(\gamma) = \gamma^4 - 2\,m\,v^2\gamma^2 + n^2 \tag{A.9}$$

We find the poles at γ as follows:

$$q(\gamma) = 0 \Longrightarrow \gamma^4 - 2\,m\,v^2\gamma^2 + n^2 = 0 \tag{A.10}$$

Thus,

$$\gamma_{1,2}^2 = m\,v^2 \pm \sqrt{(m\,v^2)^2 - n^2} \tag{A.11}$$

Assume $v^2 < n/m$ where the critical velocity is given by $v_{cr}^2 = n/m$. If $v < v_{cr}$, then

$$\begin{aligned} \gamma_{1,2}^2 &= m\,v^2 \pm i\sqrt{n^2 - (m\,v^2)^2} \\ \gamma_2^2 &= m\,v^2 - i\sqrt{n^2 - (m\,v^2)^2} \end{aligned} \tag{A.12}$$

The two roots of γ from Eq. A.12 are

$$\begin{aligned} \gamma_1 &= N + i\,M \\ \gamma_3 &= -(N + i\,M) \end{aligned} \tag{A.13}$$

where

$$\begin{aligned} M^2 + N^2 &= n \\ N^2 - M^2 &= m\,v^2 \end{aligned} \tag{A.14}$$

Solving the above system of equations, we get:

$$N = \sqrt{\frac{n + m\,v^2}{2}}, \qquad M = \sqrt{\frac{n - m\,v^2}{2}} \tag{A.15}$$

Similarly, the other two roots for γ from Eq. A.15 are

$$\begin{aligned} \gamma_2 &= -N + i\,M \\ \gamma_4 &= -(N - i\,M) \end{aligned} \tag{A.16}$$

These four poles are as shown in Fig. A–1. For $\xi(x - vt) > 0$, one considers the contour C_1 and

$$\begin{aligned} w(x,t) &= \frac{iP}{EI}\,[\mathbf{R} \text{ at } \gamma_1 + \mathbf{R} \text{ at } \gamma_2] \\ &= \frac{iP}{EI}\left[\frac{e^{i\gamma_1\xi}}{(\gamma_1-\gamma_2)(\gamma_1-\gamma_3)(\gamma_1-\gamma_4)} + \frac{e^{i\gamma_2\xi}}{(\gamma_2-\gamma_1)(\gamma_2-\gamma_3)(\gamma_2-\gamma_4)}\right] \end{aligned} \tag{A.17}$$

Now, substituting the γ_i's in terms of M and N we get:

$$w(x,t) = \frac{P\,e^{-M\xi}}{4\,E\,I\,n\,M\,N}[N\,\cos N\xi + M\,\sin N\xi] \tag{A.18}$$

Similarly for $\xi < 0$, considering the contour C_2

$$w(x,t) = \frac{P\,e^{M\xi}}{4\,E\,I\,n\,M\,N}[N\,\cos N\xi - M\,\sin N\xi] \tag{A.19}$$

APPENDIX B.
MATLAB® CODE FLOW CHART

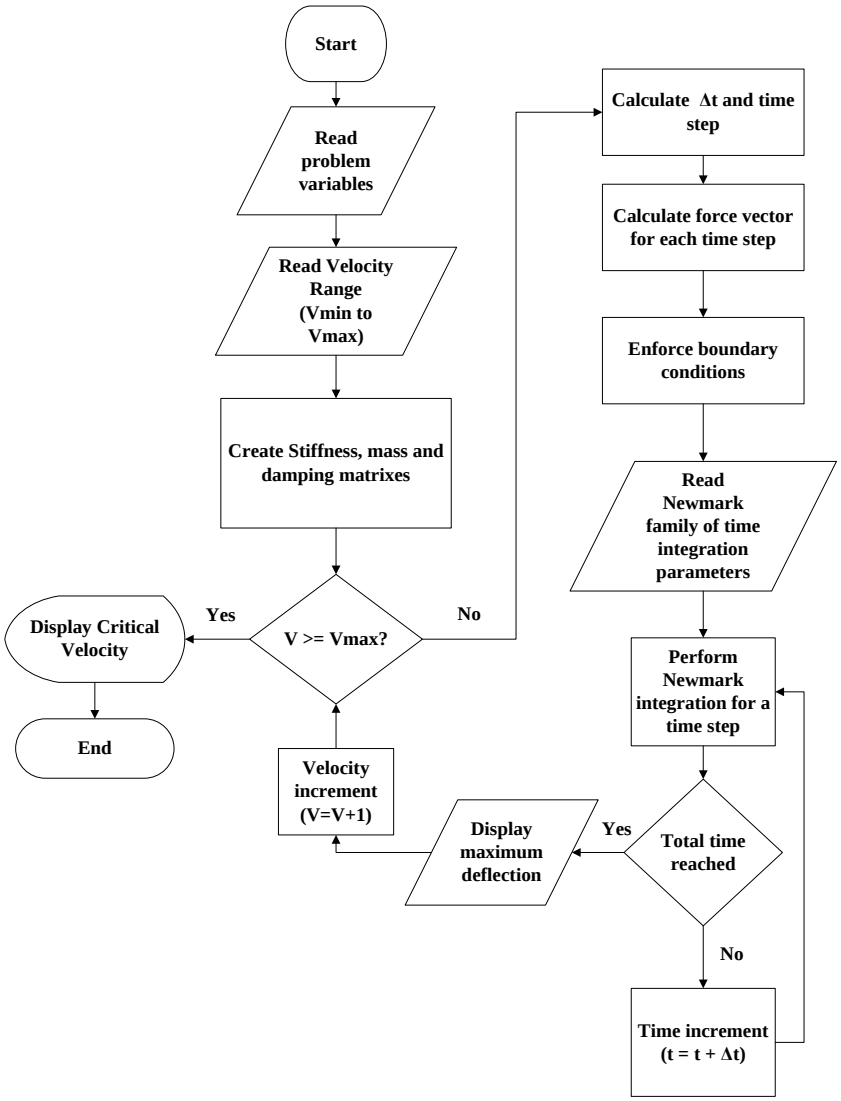

Figure B–1: Programming code flowchart.

REFERENCES

REFERENCES

[1] Timoshenko S. *"Method of Analysis of Statical and Dynamical Stresses in Rail,"* Proc. 2nd Int. Congress of Applied Mechanics, Zurich, 1927, pp. 1-12.

[2] Kenney, J.T., *"Steady-State Vibrations of Beams on Elastic foundations for Moving Load,"* Journal of Applied Mechanics, Vol. 21, No 4, Trans ASME, Vol. 76, Dec 1954, pp. 359-364.

[3] Nechitailo, N. V. and Lewis, K. B., *"Critical Velocity for Rails in Hypervelocity Launchers."* Int. J. Impact Engineering, Proc. of the Hypervelocity Impact Symposium (Lake Tahoe, CA 9-13 Oct 2005), Vol. 33, issues 1-12, Dec. 2006, p. 485-495.

[4] Jackson C.S. Yang, Coling H. Marks, Jiesheng Jiang, Decheng Chen, Aliakbar Elahi, Wen-Hu Tsai., *"Determination of Fluid Damping Using Random Excitation"* Journal of Energy Resource Technology, Trans. of the ASME, Volume 107, No. 2, pp. 220-225, 1985.

[5] A.K. Mallik, Sarvesh Chandrab and Avinash B. Sing., *"Steady-state response of an elastically supported infinite beam to a moving load "* Journal of Sound and Vibration, Vol. 291, 2006, pp. 1148-1169.

[6] McNab, I.R., Stefani, F., Crawford, M., Erengil, M., Persad, C., Satapathy, S., Vanicek, H., Watt, T., and Dampier, C., "Development of Naval Railgun," IEEE Transactions on Magnetics, Vol. 41, No. 1, Jan. 2005, pp. 206-210.

[7] Crandall, S.H., *"The Timoshenko Beam on an Elastic Foundation,"* Proceedings of the Third Midwestern Conference on Solid Mechanics, Ann Arbor, MI, 1957, pp. 146-159.

[8] Frýba,L., *"Infinite Beam on Elastic Foundation Subjected to Moving Load "* (in Czech). Aplikace matematiky, 2(1957). No. 2, 105-132.

[9] Squire, V. A., Hosking, R. J., Kerr, A. D. and Langhorne, P. J. Moving Loads on Ice Plates.Kluwer Academic Publishers, 1996.

[10] Florence, A.L., *"Traveling Force on a Timoshenko Beam,"* Journal of Applied Mechanics, Vol. 32, No 2, Trans. ASME, Vol. 87, Series E, June 1965, pp. 351-358.

[11] Achenbeck, J.D. and C.T. Sun, *"Moving Load on a Flexibly Supported Timoshenko Beam,"* International Journal of Solids and Structures, Vol. 1, 1965, pp. 353-370.

[12] Krylov, V.V., Dawson, A.R., Heelis, M.E., Collop, A.C, *"Rail Movement and Ground Waves Caused by High-speed Trains Approaching Track-soil Critical Velocities,"* Proc. Inst. Mech. Eng'rs, Part F, Journal of Rail and Rapid Transit, Vol. 214, No. 2, June 2000, pp 107-116.

[13] Steele, C.R. *"The Finite Beam With a Moving Load,"* Journal of Applied Mechanics, Vol. 34, No 1, Trans. ASME, Vol. 89, Series E, Mar. 1967, pp. 111-118.

[14] Steele, C.R. *"Nonlinear Effects in the Problem of a Beam on a Foundation With Moving Load,"* International Journal of Solids and Structures, Vol. 3, No 4, July 1967, pp. 565-585.

[15] Steele, C.R. *"The Timoshenko Beam With a Moving Load,"* Journal of Applied Mechanics, Vol. 35, No 3, Trans. ASME, Vol. 90, Sept. 1968, pp. 481-488.

[16] Wu YS,Yang YB, *"A semi-analytical approach for analyzing ground vibrations caused by trains moving over elevated bridges,"* Soil Dynamics and Earthquake Engineering 2004, Vol.24, pp. 949962.

[17] Frýba, L., *"A rough assessment of railway bridges for high speed trains,"*. Engineering Structures, 2001, Vol. 23 pp. 548556.

[18] Frýba, L., *"Impacts of Two-Axle System Traversing a Beam,"*. International Journal of Solids and Structures, 1968. Vol.4 , pp. 1117-1123.

[19] Frýba, L., Pirner, M. *"Load tests and modal analysis of bridges,"*. Engineering Structures, 2001, Vol.23, pp. 102109.

[20] Frýba, L., Yau, J.D., *"Suspended Bridges Subjected to Moving Loads and Support Motions due to Earthquake,"*. Journal of Sound and Vibration, 2009 Vol.319. pp. 218227.

[21] Paolucci, R., Maffeis, A., Scandella, L., Stupazzini,M., Vanini, M. *"Numerical Prediction of Low-Frequency Ground Vibrations Induced by High-Speed Trains at Ledsgaard, Sweden,"*.Soil Dynamics and Earthquake Engineering, 2003, Vol. 23 pp. 425433.

[22] Banimahd, M., Woodward, P.K., *"Numerical Study of Train Speed Effect on Railway Track Response,"*. Proceeding of 9th International COnference on Railway Engineering, London, June, 2007.

[23] Stanisic, M.M., Hardin, J.C., and Lou, Y.C., *"On the response of a plate to a multi-Masses moving System",* Acta Mechanica, Vol.5, 1968, pp. 37-53.

[24] Fryba, L. *"Vibrations of Solids and Structures under Moving Loads,"* Thomas Telford, 1999.

[25] Seong-Min Kim and Jose M. Roesset *"Dynamic Response of a Beam on a Frequency-Independent Damped Elastic Foundation to Moving Load,"*Canadian Journal of Civil Engineering, Vol. 30, No 2, Apr. 2003, ProQuest Science Journals, pp. 460 - 467.

[26] L. Andersen, S. R. K. Nielsen AND P. H. Kirkegaard *"Finite Element Modelling of Infinite EulerBeams on Kelving Foundations Exposed to Moving Loads in Convected Co-Ordinates"* Journal of Sound and Vibration, Vol. 241, No 4, 2001, pp. 587-604.

[27] Taheri, M. R., and Ting, E. C. *"Dynamic Response of Plate to Moving Loads:Structural Impedance Method,"* Computers and Structures, Vol. 33, No 6, 1989, pp. 1379-1393.

[28] Taheri, M. R., and Ting, E. C. *"Dynamic Response of Plate to Moving Loads:Finite Element Method,"* Computers and Structures., Vol. 34, No 3, 1990, pp. 509-521.

[29] Gbadeyan, J. A., and Oni, S. T. *"Dynamic Response to Moving Concentrated Masses of Elastic Plates on a Non-Winkler Elastic Foundation,"* Journal of Sound and Vibration, Vol. 154, No 2, April 1992, pp. 343-358.

[30] Gbadeyan, J. A., and Oni, S. T. *"Dynamic Behaviour of Beams and Rectangular Plates under Moving Loads",* Journal of Sound and Vibration, Vol. 182, No 5,

1995, pp. 677-695.

[31] Kim, S. M., and Roesset, J. M. *"Moving loads on a plate on elastic foundation,"* J. Eng. Mech., Vol. 124, No 9, Sept. 1998, pp. 1010-1017.

[32] Kim, S. M., and McCullough, B.F. *"Dynamic response of plate on viscous Winkler foundation to moving loads of varying amplitude"* Engineering Structures, Vol.25, 2003, pp. 11791188.

[33] Huang, M. H., and Thambiratnam, D. P. *"Dynamic Response of Plates on Elastic Foundation to Moving Loads,"* J. Eng. Mech., Sept. 2002, Vol. 128, No 9, pp. 1016-1022.

[34] Kim, S. M.,*"Buckling and vibration of a plate on elastic foundation subjected to in-plane compression and moving loads,"* International Journal of Solids and Structures, Vol. 41, 2004, pp. 56475661.

[35] Sun, L., *"Analytical dynamic displacement response of rigid pavements to moving concentrated and line loads,"* International Journal of Solids and Structures, Vol.43, 2006, pp. 43704383.

[36] Yagiz, N. and Sakman, L.E., *"Vibrations of a Rectangular Bridge as an Isotropic Plate under a Traveling Full Vehicle Model,"* Journal of Vibration and Control, Vol.12(1), 2006, pp. 8398.

[37] Law, S.S., Bu, J.Q., Zhu, X.Q., and Chan, S.L., *"Moving load identification on a simply supported orthotropic plate,"* International Journal of Mechanical Sciences Vol.49, 2007, pp. 12621275.

[38] Livesley, R. K., *"Some notes on the mathematical theory of a loaded elastic plate resting on a elastic foundation,"* The Quartely Journal of Mechanics and Applied Mathematics, 1953, pp.32-44.

[39] Hsi-Ming Pan, *"Transient analysis of a plate on an elastic foundation under a moving load, "* Ph. D Dissertation, Stanford University, 1987.

[40] Bilello, M.A., *"Maximum thickness and subsequent decay of lake, river and fast sea ice in Canada and Alaska,"* U.S. Army Cold Regions Research and Engineering Laboratory, 1980, Hanover, N.H., CRREL Report 80-6.

[41] Wilson, J.T., *"Coupling between moving loads and flexural waves in floating ice sheets "* US Army *SIPRE* Report 34, 1955, Cold Regions Research and Engineering Laboratory, Hanover, New Hampshire, U.S.A.

[42] Wilson, J.T., *"Moving loads on floating ice sheets,"* Univeristy of Michigan Research Institute Report, 1958, Project 2432, Michigan, U.S.A.

[43] Sunberg-Falkenmark, M., *"Resultat av belastningsförsök på is, utförda av Samarbetsgruppen för isbärighetsförsök "* (in Swedish). Notiser Och Preliminära Rappoter, Serie Hydrologi 1, 1963, Sveriges Meteorologiska och Hydrologiska Institut, Stockholm, Sweden.

[44] Beltaos, S., *"Field studies on the response of floating ice sheets to moving loads,"* No 8, Canadian Journal of Civil Engineering, 1981, pp. 1-8.

[45] Traetterberg, A., Gold, L.W., Frederking, R., *"Strain rate and temperature dependence of Young's modulus of ice "* IAHR, 1975, pp. 479-486.

[46] Mellor, M.,*"Mechanical behaviour of sea ice,"* CRREL Monograph 83-1, 1983, Cold Regions Research and Engineering Laboratory, Hanover, New Hampshire, U.S.A.

[47] Zhuchao, YE., Huaihai, CHEN, *"Vibration analysis of a simply supported beam under moving mass based on moving finite element method "*Mech. Eng. China, 2009, Vol.4, No.4, pp. 397400.

[48] Jia-Jang, Wu., Whittaker, A.R., Cartmell, M.P. *"The use of finite element techniques for calculating the dynamic response of structures to moving loads "*Computers and Structures Vol.78, 2000, pp. 789-799.

[49] Reddy, J. N., *"An Introduction to the Finite Element Method,"* McGraw-Hill Book Company, 1993, New York, N.Y.

[50] Ashton, George D.,*"River Lake Ice Engineering,"* Water Resources Publications, LLC., 2010, Highlands Ranch, Colorado.

[51] Potter, Merle C., Wiggert, David C. with Hondzo, Midhat., *"Mechanics of Fluids,"* Prentice Hall, 1997, Upper Saddle River, N.J.

[52] Hetényi M., *"Beams on Elastic Foundation: Theory with Applications in the Fields of Civil and Mechanical Engineering"*. Univ. of Michigan Press, Ann Arbor, Michigan, 1964.

[53] Goyal, Vijay K. and Goyal, V.K., *"Aircraft Structures for Engineers"* 2012, Pearson Education Publisher (under revision), N.J.

[54] Goyal, Vijay K. and Goyal, V.K., *"Finite Element Analysis"* 2012, Pearson Education Publisher (under revision), N.J.

[55] *https://www.usrbc.org*

APPENDIX C.
BIOGRAPHICAL SKETCH OF ÁNGEL QUINTERO

Ángel Luis Quintero-Cartagena was born in Puerto Rico and is bilingual in both English and Spanish, with over 8 years of experience with finite element methods. He completed his bachelor degree in Mechanical Engineering at the University of Puerto Rico at Mayagüez. During his undergraduate studies, Angel mainly focused in the use of finite element analysis software packages (e.g. ANSYS, ABAQUS and NASTRAN) for the thermal and structural applications and MATLAB programming. His main areas of research include: structures, vibrations, dynamic stability analysis, time-dependent finite element analysis and HVAC design.

He joined the master's program in Mechanical Engineering at the University of Puerto Rico at Mayagüez in August of 2006 while working for the pharmaceutical and medical device companies, serving the United States and Latin-American countries. His focus in these companies was in new product development. Angel has been the leader in the area of product manufacturing characterization, regulatory submissions and product transfer for multinational companies. Also, Angel has worked as a Six Sigma mentor and is a Six Sigma Black Belt certified. His expertise includes but are not limited to supervision and people management, process excellence, project management and regulatory affairs.

FINITE ELEMENT ANALYSIS OF UNEXPECTED FAILURE OF LAKE-ICE UNDER LOADS MOVING AT CRITICAL VELOCITY

Ángel L. Quintero Cartagena

(787) 832-4040

Department of Mechanical Engineering

Chair: Vijay K. Goyal

Degree: Master of Science

Graduation Date: July 2012